

Charged anti-de Sitter scalar-tensor black holes and their thermodynamic phase structure

Daniela D. Doneva^{1,2*}, Stoytcho S. Yazadjiev^{3 †}, Kostas D. Kokkotas^{2,4 ‡}

¹Dept. of Astronomy, Faculty of Physics, St.Kliment Ohridski University of Sofia
5, James Bourchier Blvd., 1164 Sofia, Bulgaria

²Theoretical Astrophysics, Eberhard-Karls University of Tübingen, Tübingen 72076, Germany

³Dept. of Theoretical Physics, Faculty of Physics, St.Kliment Ohridski University of Sofia
5, James Bourchier Blvd., 1164 Sofia, Bulgaria

⁴Department of Physics, Aristotle University of Thessaloniki, Thessaloniki 54124, Greece

Ivan Zh. Stefanov^{5 §}, Michail D. Todorov^{6 ¶}

⁵Department of Applied Physics, Technical University of Sofia,
8, Kliment Ohridski Blvd., 1000 Sofia, Bulgaria

⁶Faculty of Applied Mathematics and Computer Science, Technical University of Sofia
8, Kliment Ohridski Blvd., 1000 Sofia, Bulgaria

Abstract

In the present paper we numerically construct new charged anti-de Sitter black holes coupled to nonlinear Born-Infeld electrodynamics within a certain class of scalar-tensor theories. The properties of the solutions are investigated both numerically and analytically. We also study the thermodynamics of the black holes in the canonical ensemble. For large values of the Born-Infeld parameter and for a certain interval of the charge values we find the existence of a first-order phase transition between small and very large black holes. An unexpected result is that for a certain small charge subinterval two phase transitions have been observed, one of zeroth and one of first order. It is important to note that such phase transitions are also observed for pure Einstein-Born-Infeld-AdS black holes.

PACS: 04.50.Kd; 04.70.Bw; 04.25.D

*E-mail: ddoneva@phys.uni-sofia.bg

†E-mail: yazad@phys.uni-sofia.bg

‡E-mail: kostas.kokkotas@uni-tuebingen.de

§E-mail: izhivkov@yahoo.com

¶E-mail: mtod@tu-sofia.bg

1 Introduction

In the last decade anti-de Sitter (AdS) black holes and especially their thermodynamics have attracted considerable interest due to the AdS/CFT duality. According to the AdS/CFT conjecture the thermodynamics of the AdS black holes is related to the thermodynamics of the dual conformal field theory (CFT) residing on the boundary of the AdS space [1, 2]. In their pioneering work Hawking and Page [3] showed the existence of a phase transition between the AdS black hole and thermal AdS space. The AdS/CFT duality provides us with a new tool to study the phase transitions in the dual CFT theories on the base of studying the phase transitions of the AdS black holes.

Charged AdS black holes and their thermodynamics have been studied not only within the linear Maxwell electrodynamics but also within the framework of the nonlinear electrodynamics of Born-Infeld. This nonlinear electrodynamics was first introduced by Born and Infeld in 1934 as an attempt to obtain a finite energy density model for the electron [4]. The interest for nonlinear electrodynamics has been later revived in the context of string theory. It arises naturally in open strings and D-branes [5] – [8]. Nonlinear electrodynamics models coupled to gravity have been discussed in different aspects (see, for example, [9] – [20] and references therein). In particular, black holes coupled to Born-Infeld electrodynamics, including in the presence of a cosmological constant, have been studied in numerous papers [17],[21] – [40], and their thermodynamics in [41] – [44].

The aim of the present paper is to study the charged AdS black holes coupled to nonlinear Born-Infeld electrodynamics and their thermodynamics within the framework of a certain class of scalar-tensor theories (STT). Scalar-tensor theories of gravity are among the most natural generalizations of general relativity (GR) and arise in string theory and higher dimensional gravity theories [45]. The fundamental question is whether objects found and studied in the frame of GR, such as black holes, would have different properties in the frame of the scalar-tensor theories. Recent studies on asymptotically flat, scalar-tensor black holes coupled to nonlinear electrodynamics show that the presence of a scalar field in the gravitational sector leads to interesting and serious consequences for the black holes. In the general case the scalar field restricts the possible causal structures in comparison to the pure Einstein gravity [38, 39]. For some classes of scalar-tensor theories [46] there even exist non-unique scalar-tensor black hole solutions with the same conserved asymptotic charges. In other words the spectrum of asymptotically flat black hole solutions coupled to nonlinear electrodynamics in the STT is much richer and much more complicated than in general relativity. This shows that the scalar-tensor black holes coupled to nonlinear electrodynamics and other sources with non-vanishing trace of the energy-momentum tensor (in four dimensions) constitute an area that deserves further study. In view of the current great interest in the AdS black holes, the natural next step is to study the scalar-tensor black holes coupled to nonlinear electrodynamics in spacetimes with AdS asymptotic.

In this paper we construct new numerical solutions describing charged AdS scalar-tensor black holes coupled to nonlinear Born-Infeld electrodynamics and we make a parameter study of their properties. The thermodynamics of the constructed solutions

in canonical ensemble is also studied. We found that for large values of the Born-Infeld parameter b and for a certain interval of intermediate values of the charge there exist a first-order phase transition between small and very large black holes. An interesting result is that for a small subinterval one more phase transition exists which is of zeroth order since the thermodynamic potential is discontinuous there – it jumps to a lower value. Such phase transition of first and zeroth order can be observed also in pure Einstein gravity, i.e. when no scalar field is present.

The phase structure of the Einstein-Born-Infeld black holes and the possible Hawking-Page transitions have been examined in [41] and [47]. Hawking-Page phase transitions have been studied for different black holes, for example, Einstein-Maxwell black holes in spacetime with different dimensions [48, 49], in three-dimensional spacetime [50, 51], in higher-derivative gravity [52, 53], in higher-curvature gravity [54], and in unusual electrodynamics which does not restore the Maxwell electrodynamics in the weak-field limit [55]. Phase transitions between solitons and black holes in asymptotically AdS/ \mathbb{Z}_k spaces have been studied in [56].

2 Formulation of the problem

The most general form of the action in scalar-tensor theories is

$$S = \frac{1}{16\pi G_*} \int d^4x \sqrt{-\tilde{g}} \left(F(\Phi) \tilde{R} - Z(\Phi) \tilde{g}^{\mu\nu} \partial_\mu \Phi \partial_\nu \Phi - 2U(\Phi) \right) + S_m[\Psi_m; \tilde{g}_{\mu\nu}], \quad (1)$$

where G_* is the bare gravitational constant and \tilde{R} is the Ricci scalar curvature with respect to the spacetime metric $\tilde{g}^{\mu\nu}$. $F(\Phi)$, $Z(\Phi)$, and $U(\Phi)$ are functions of the scalar field Φ and their specific choice determines the scalar-tensor theory completely. In order for the gravitons to carry positive energy the function $F(\Phi)$ must be positive ($F(\Phi) > 0$), while the non-negativity of the scalar field energy requires that $2F(\Phi)Z(\Phi) + 3[dF(\Phi)/d\Phi]^2 \geq 0$. The action of the sources is $S_m[\Psi_m; \tilde{g}_{\mu\nu}]$ and there is no direct coupling between the sources of gravity and the scalar field in order for the weak equivalence principle to be satisfied.

The action (1) is in the so called Jordan frame which is the physical frame but it is more convenient to work in the Einstein frame. The relations between the two frames are

$$g_{\mu\nu} = F(\Phi) \tilde{g}_{\mu\nu}, \quad (2)$$

$$\left(\frac{d\varphi}{d\Phi} \right)^2 = \frac{3}{4} \left(\frac{d \ln(F(\Phi))}{d\Phi} \right)^2 + \frac{Z(\Phi)}{2F(\Phi)}, \quad (3)$$

where $g_{\mu\nu}$ and φ are correspondingly the metric and the scalar field in the Einstein frame. The additional introduction of the functions

$$\mathcal{A}(\varphi) = F^{-1/2}(\Phi), \quad (4)$$

$$V(\varphi) = \frac{1}{2} U(\Phi) F^{-2}(\Phi), \quad (5)$$

leads to the following action in the Einstein frame:

$$S = \frac{1}{16\pi G_*} \int d^4x \sqrt{-g} (R - 2g^{\mu\nu} \partial_\mu \varphi \partial_\nu \varphi - 4V(\varphi)) + S_m[\Psi_m; \mathcal{A}^2(\varphi)g_{\mu\nu}], \quad (6)$$

where R is the Ricci scalar curvature with respect to the spacetime metric $g_{\mu\nu}$. In the Einstein frame there is direct coupling between the sources of gravity and the scalar fields through the coupling function $\mathcal{A}(\varphi)$ and the specific choice of the scalar-tensor theory is completely determined by this function and by the potential of the scalar field $V(\varphi)$.

Here we will consider nonlinear electrodynamics and its action in the Einstein frame is given by

$$S_m = \frac{1}{4\pi G_*} \int d^4x \sqrt{-g} \mathcal{A}^4(\varphi) L(X, Y), \quad (7)$$

where $L(X, Y)$ is the Lagrangian of the nonlinear electrodynamics. The equations defining the functions X and Y are

$$X = \frac{\mathcal{A}^{-4}(\varphi)}{4} F_{\mu\nu} F^{\mu\nu}, \quad (8)$$

$$Y = \frac{\mathcal{A}^{-4}(\varphi)}{4} F_{\mu\nu} (\star F)^{\mu\nu}, \quad (9)$$

where $F_{\mu\nu}$ is the electromagnetic field strength tensor and \star stands for the Hodge dual with respect to the metric $g_{\mu\nu}$.

The Lagrangian of the Born-Infeld nonlinear electrodynamics is

$$L = 2b \left[1 - \sqrt{1 + \frac{X}{b} - \frac{Y^2}{4b^2}} \right], \quad (10)$$

where b is a parameter and in the limit $b \rightarrow \infty$ the linear Maxwell electrodynamics is restored.

The variation of the action (6) leads to the following field equations

$$\begin{aligned} R_{\mu\nu} &= 2\partial_\mu \varphi \partial_\nu \varphi + 2V(\varphi)g_{\mu\nu} - 2\partial_X L(X, Y) \left(F_{\mu\beta} F_\nu^\beta - \frac{1}{2}g_{\mu\nu} F_{\alpha\beta} F^{\alpha\beta} \right) \\ &\quad - 2\mathcal{A}^4(\varphi) [L(X, Y) - Y\partial_Y L(X, Y)] g_{\mu\nu}, \\ \nabla_\mu [\partial_X L(X, Y) F^{\mu\nu} + \partial_Y L(X, Y) (\star F)^{\mu\nu}] &= 0, \end{aligned} \quad (11)$$

$$\nabla_\mu \nabla^\mu \varphi = \frac{dV(\varphi)}{d\varphi} - 4\alpha(\varphi) \mathcal{A}^4(\varphi) [L(X, Y) - X\partial_X L(X, Y) - Y\partial_Y L(X, Y)],$$

where

$$\alpha(\varphi) = \frac{d \ln \mathcal{A}(\varphi)}{d\varphi}. \quad (12)$$

In the present paper we are interested in spacetimes with anti-de Sitter asymptotic structure and thus we will consider the following type of potential:

$$V = \frac{1}{2}\Lambda, \quad (13)$$

where $\Lambda < 0$ is a constant. The coefficient $1/2$ is a standard normalizing factor.

Let us explain the reasons for choosing the potential (13). For this purpose we consider the Jordan frame and we require the metric to have AdS asymptotic¹ in this frame. Then we have two possibilities – either the factor $F(\Phi)$ is finite at infinity (i.e. $0 < F(\Phi_\infty) < \infty$) or it is divergent at infinity. Although the case when $F(\Phi)$ is divergent at infinity could be of some interest, it is not generic and in fact is degenerate since it corresponds to zero effective gravitational constant at infinity. Here we consider only "physically well-behaved" solutions with finite² $F(\Phi_\infty) > 0$. Using the (Jordan frame) field equations and especially the equation for Φ , one can show that the finiteness of $F(\Phi)$ at infinity requires

$$\lim_{\Phi \rightarrow \Phi_\infty} \left[\frac{\frac{dU(\Phi)}{d\Phi} F(\Phi) - 2U(\Phi) \frac{dF(\Phi)}{d\Phi}}{2Z(\Phi)F(\Phi) + 3 \left(\frac{dF(\Phi)}{d\Phi} \right)^2} \right] = \lim_{\Phi \rightarrow \Phi_\infty} \left[\frac{F^3(\Phi) \frac{d}{d\Phi} \left(\frac{U(\Phi)}{F^2(\Phi)} \right)}{2Z(\Phi)F(\Phi) + 3 \left(\frac{dF(\Phi)}{d\Phi} \right)^2} \right] = 0, \quad (14)$$

$$\lim_{\Phi \rightarrow \Phi_\infty} U(\Phi) = \Lambda.$$

The simplest (Jordan frame) potential satisfying this condition³, i.e. allowing simultaneously AdS asymptotic for the metric and finite $F(\Phi_\infty) > 0$, is $U(\Phi) = \Lambda F^2(\Phi)/F^2(\Phi_\infty)$ which corresponds exactly to the Einstein frame potential (13) for $F(\Phi_\infty) = 1$. The conditions (14) written in the Einstein frame take the form

$$\lim_{\varphi \rightarrow \varphi_\infty} \frac{dV(\varphi)}{d\varphi} = 0, \quad \lim_{\varphi \rightarrow \varphi_\infty} V(\varphi) = \frac{1}{2}\Lambda. \quad (15)$$

From here it is obvious that $V(\varphi) = \Lambda/2$ is indeed the simplest choice of a potential admitting the desired properties.

One can show, as we shall see below, that for the scalar-tensor theories under consideration, the asymptotic behavior of the factor $F(\Phi)$ is $F(\Phi) \approx 1 + \text{const}/r^3$ and it guarantees the same anti-de Sitter asymptotic structure simultaneously in both the Jordan and the Einstein frames. Moreover, the asymptotic behavior of $F(\Phi)$ guarantees that the mass of the Jordan frame solution is the same as that of the Einstein frame solution. This can be easily seen from the results in Appendix B.

¹We mean AdS asymptotic corresponding to a cosmological term Λ .

²Throughout this paper, without loss of generality, we set $F(\Phi_\infty) = 1$.

³More precisely, we mean the simplest potential in the framework of the class of scalar-tensor theories considered in the present paper. For this class of scalar-tensor theories the denominator in (14) is finite.

Another reason for considering finite $F(\Phi_\infty)$ comes from the thermodynamics. The black hole thermodynamics in scalar-tensor theories is naturally defined in the Einstein frame as discussed in Appendix A. When $F(\Phi)$ is divergent at infinity the conformal transformation does not preserve the AdS asymptotic when we move from the Jordan to the Einstein frame. In this case the expected thermodynamic would be rather different from that of the AdS black holes if it could be defined at all because of the rather unusual spacetime asymptotic.

3 Basic equations

3.1 The reduced system

Here and below we will work in a system of units in which $G_* = c = \mu_0/4\pi = 1$, where μ_0 is the magnetic permeability of the vacuum. In this system

$$[P] = m; \quad [M] = m; \quad [b] = m^{-2}.$$

We will consider a static and spherically symmetric spacetime and the ansatz for the metric (in the Einstein frame) is

$$ds^2 = g_{\mu\nu} dx^\mu dx^\nu = -f(r)e^{-2\delta(r)} dt^2 + \frac{dr^2}{f(r)} + r^2 (d\theta^2 + \sin^2 \theta d\phi^2). \quad (16)$$

An important property of the Born-Infeld electrodynamics is the electric-magnetic duality symmetry of the theory [57] – [61]. It is sufficient to study only the magnetically charged case, and the electrically charged solution can be obtained from the magnetically charged solution using the electric-magnetic rotation defined by

$$\{g_{\mu\nu}, \varphi, F_{\mu\nu}, P, X, L(X)\} \longleftrightarrow \{g_{\mu\nu}, \varphi, \star G_{\mu\nu}, \bar{Q}, \bar{X}, L(\bar{X})\}, \quad (17)$$

where the functions denoted by $(\bar{\cdot})$ correspond to the dual solution, P is the magnetic charge, \bar{Q} is the charge of the dual solution, and

$$G_{\mu\nu} = -2 \frac{\partial [\mathcal{A}^4(\varphi)L]}{\partial F^{\mu\nu}}, \quad \bar{X} = -\left[\partial_X L(X)\right]^2 X. \quad (18)$$

In the magnetically charged case the electromagnetic field strength tensor is

$$F = P \sin \theta d\theta \wedge d\phi, \quad (19)$$

where P is the magnetic charge. For the functions X and Y we obtain

$$X = \frac{\mathcal{A}^{-4}(\varphi) P^2}{2 r^4}, \quad Y = 0. \quad (20)$$

The truncated Born-Infeld Lagrangian is

$$L(X) = 2b \left(1 - \sqrt{1 + \frac{X}{b}} \right). \quad (21)$$

Using the metric (16) the field equations reduce to the following system of coupled ordinary differential equations

$$f'' - 2f\delta'' - 3f'\delta' + 2f\delta'^2 + \frac{2}{r}f' - \frac{4}{r}f\delta' = -4 \{V(\varphi) + \mathcal{A}^4(\varphi) [2X\partial_X L(X) - L(X)]\}, \quad (22)$$

$$f'' - 2f\delta'' - 3f'\delta' + 2f\delta'^2 + \frac{2}{r}f' = -4 \{f\varphi'^2 + V(\varphi) + \mathcal{A}^4(\varphi) [2X\partial_X L(X) - L(X)]\}, \quad (23)$$

$$1 - f - rf' + rf\delta' = 2r^2 [V(\varphi) - \mathcal{A}^4(\varphi)L(X)], \quad (24)$$

$$\frac{d}{dr} \left(e^{-\delta} r^2 f \frac{d\varphi}{dr} \right) = \frac{dV(\varphi)}{d\varphi} e^{-\delta} r^2 + 4r^2 e^{-\delta} \alpha(\varphi) \mathcal{A}^4(\varphi) [X\partial_X L(X) - L(X)]. \quad (25)$$

These are four equations for only three unknown functions f , φ and δ but the self-consistency of the system is guaranteed by the Bianchi identity.

In pure Einstein theory the solution describing Schwarzschild-AdS black holes is

$$\delta_E(r) = 0, \quad (26)$$

$$f_E(r) = 1 - \frac{2M_E}{r} - \frac{1}{3}\Lambda r^2, \quad (27)$$

where M_E is the mass of the black hole. The asymptotic of the metric function $f(r)$ at infinity in our problem is the same ($-\frac{1}{3}\Lambda r^2$) and this means that $f(r)$ is unbounded at infinity. From a numerical point of view it is convenient to introduce a new unknown function $m(r)$ (which is finite at infinity in the considered class of theories) using the substitution

$$f(r) = 1 - \frac{2m(r)}{r} - \frac{1}{3}\Lambda r^2. \quad (28)$$

Using the system (22)-(25) after some manipulations we can obtain the following simpler system of ordinary differential equations

$$\frac{d\delta}{dr} = -r \left(\frac{d\varphi}{dr} \right)^2, \quad (29)$$

$$\frac{dm}{dr} = r^2 \left[\frac{1}{2} f \left(\frac{d\varphi}{dr} \right)^2 - \mathcal{A}(\varphi)^4 L(X) \right], \quad (30)$$

$$\frac{d}{dr} \left(r^2 f \frac{d\varphi}{dr} \right) = r^2 \left\{ -4\alpha(\varphi) \mathcal{A}^4(\varphi) [L - X\partial_X L(X)] - r f \left(\frac{d\varphi}{dr} \right)^3 \right\}. \quad (31)$$

The first equation (29) is decoupled and it can be solved separately once a solution for the functions $m(r)$ and $\varphi(r)$ is obtained.

We will consider a class of scalar-tensor theories for which $\alpha(\varphi) = \text{const} \equiv \alpha > 0^4$. The investigation of the case with $\alpha(\varphi) = \text{const} \equiv \alpha < 0$ is similar. Although we restrict ourselves to $\alpha(\varphi) = \text{const} \equiv \alpha$ the obtained results are qualitatively⁵ the same even for more general coupling functions $\alpha(\varphi) > 0$ for which $\alpha(0) = \alpha$.

In the chosen ansatz for the metric (16) the temperature is given by the following relation

$$T = \left. \frac{f'(r) e^{-\delta(r)}}{4\pi} \right|_{r=r_H}. \quad (32)$$

3.2 Asymptotic behavior

The asymptotic behavior of the functions δ , m and φ at $r \rightarrow \infty$ is

$$\delta|_{r \rightarrow \infty} = \frac{3C_3^2}{2r^6} + \mathcal{O}(r^{-8}), \quad (33)$$

$$m|_{r \rightarrow \infty} = M - \frac{P^2}{2r} + \frac{\Lambda C_3^2}{2r^3} + \mathcal{O}(r^{-5}), \quad (34)$$

$$\varphi|_{r \rightarrow \infty} = \frac{C_3}{r^3} + \frac{9C_3}{5\Lambda r^5} - \frac{3MC_3}{\Lambda r^6} + \mathcal{O}(r^{-7}), \quad (35)$$

where C_3 is a constant and M is the mass of the black hole in the Einstein frame (for the definition of the mass in the AdS spaces see Appendix A). Let us compare the asymptotic behavior of these functions in AdS and in asymptotically flat spacetime. In AdS spacetime the scalar field decreases as $1/r^3$ and this is much faster than in the asymptotically flat case where the scalar field decreases as $1/r$. The function $\delta(r)$ also decreases much faster in AdS spacetime, where the leading term is proportional to $1/r^6$ compared to the leading term $1/r^2$ in the asymptotically flat spacetime. The asymptotic behavior of $m(r)$ up to first order in $1/r$ is the same.

3.3 Qualitative properties

We can obtain some information for the black hole solutions using equations (25) and (29) and the boundary conditions. We prove that the black holes under consideration have simpler causal structure than the black holes in pure Einstein-Born-Infeld theory in AdS spacetime and we also obtained some information for the behavior of the unknown functions. The general properties of the considered scalar-tensor black holes coupled to Born-Infeld nonlinear electrodynamics in AdS spacetime can be summarized as follows:

1. The black holes have only one event horizon and extremal black holes do not exist.
2. The scalar field φ is negative on the event horizon, it has no zeros and increases monotonically.

⁴Constant $\alpha(\varphi)$ corresponds to Brans-Dicke scalar-tensor theory.

⁵As the numerical results show the picture is not only qualitatively but also quantitatively close for all scalar-tensor theories with the same $\alpha(0)$.

3. The metric function δ is positive on the event horizon, it has no zeros and decreases monotonically.

To prove these statements we should first note that it can be easily shown that for the Born-Infeld electrodynamics the following inequality is satisfied:

$$X\partial_X L(X) - L(X) > 0. \quad (36)$$

We will first prove that the considered black holes have only one horizon. Let us assume that they have two horizons r_- and r_+ , where $r_+ > r_-$. When we integrate equation (25) in the interval $r \in [r_-, r_+]$ we obtain

$$\begin{aligned} & \left(e^{-\delta} r^2 f \frac{d\varphi}{dr} \right) \Big|_{r_+} - \left(e^{-\delta} r^2 f \frac{d\varphi}{dr} \right) \Big|_{r_-} = \\ & = 4 \int_{r_-}^{r_+} r^2 e^{-\delta} \alpha(\varphi) \mathcal{A}^4(\varphi) [X\partial_X L(X) - L(X)] dr > 0. \end{aligned} \quad (37)$$

The horizons are defined as the points where $f(r) = 0$ so the left-hand side of the equation is zero. But from (36) and the fact that we consider $\alpha(\varphi) > 0$ it is obvious that the right-hand side is strictly positive. So we reached a contradiction and this means that two black hole horizons cannot exist.

In order to prove that an extremal black hole cannot exist we will examine again equation (25), that is

$$\frac{d}{dr} \left(e^{-\delta} r^2 f \frac{d\varphi}{dr} \right) = 4r^2 e^{-\delta} \alpha(\varphi) \mathcal{A}^4(\varphi) [X\partial_X L(X) - L(X)] > 0.$$

Let us assume that we have a degenerate event horizon at r_d . The right-hand side of the equation is strictly positive for every $r_d > 0$,⁶ but the left-hand side is zero and we reach a contradiction.

We can investigate the behavior of the function $\varphi(r)$ in the domain $r \in [r_H, \infty)$ (r_H is the radius of the event horizon) using equation (25). As we already noted the right-hand side of (25) is positive. Integration of equation (25) from r_H to $r > r_H$ gives

$$e^{-\delta} r^2 f(r) \frac{d\varphi}{dr} = 4 \int_{r_H}^r r^2 e^{-\delta} \alpha(\varphi) \mathcal{A}^4(\varphi) [X\partial_X L(X) - L(X)] dr > 0. \quad (38)$$

This shows that $d\varphi/dr > 0$ in the domain (r_H, ∞) . Therefore $\varphi(r)$ increases monotonically. Since the asymptotic value of the scalar field at infinity is zero we can conclude that φ should be negative on the horizon and monotonically increasing to zero. From (38) taking the limit $r \rightarrow \infty$ we find that $C_3 < 0$.

Finally, $\delta(r)$ decreases monotonically since the right-hand side of equation (29) is always negative. The asymptotic value of $\delta(r)$ at infinity is zero so we can conclude that it is positive on the event horizon and monotonically decreasing to zero.

All of the above presented propositions remain valid for different nonlinear electrodynamics for which the relation (36) holds.

⁶We are not interested in the case $r_d = 0$ because this corresponds to naked singularity.

3.4 Dimensionless quantities

The reduced field equations (29)–(31) are invariant under the rigid rescaling

$$r \rightarrow \lambda r, \quad m \rightarrow \lambda m, \quad \Lambda \rightarrow \lambda^{-2}\Lambda, \quad b \rightarrow \lambda^{-2}b, \quad P \rightarrow \lambda P. \quad (39)$$

Therefore, one may generate in this way a family of new solutions. Thus, the mass, the temperature and the entropy of the new solutions are given by the formulas

$$M \rightarrow \lambda M, \quad T \rightarrow \lambda^{-1}T, \quad S \rightarrow \lambda^2 S. \quad (40)$$

As a consequence of the rigid symmetry we may restrict our study to the case $\Lambda = -1$ by introducing the dimensionless quantities

$$\begin{aligned} r &\rightarrow \frac{r}{l}, \quad m \rightarrow \frac{m}{l}, \quad b \rightarrow bl^2, \quad P \rightarrow \frac{P}{l}, \\ M &\rightarrow \frac{M}{l}, \quad T \rightarrow lT, \quad S \rightarrow \frac{S}{l^2}, \end{aligned} \quad (41)$$

where the choice of $\Lambda = -1$ requires

$$l = \frac{1}{\sqrt{-\Lambda}}. \quad (42)$$

3.5 Posing the Boundary-Value Problem

The domain of integration is half-infinite $r \in [r_H, \infty)$ where the horizon, which is the left boundary, is *a priori* unknown. We impose the following boundary conditions:

— At infinity:

$$\lim_{r \rightarrow \infty} m(r) = M, \quad (43)$$

$$\lim_{r \rightarrow \infty} \delta(r) = \lim_{r \rightarrow \infty} \varphi(r) = 0, \quad (44)$$

where M is the mass of the black hole in the Einstein frame (see Appendix A);

— On the horizon:

$$f(r_H) = 0. \quad (45)$$

The following regularization condition should also be fulfilled on the horizon:

$$\left. \frac{df}{dr} \cdot \frac{d\varphi}{dr} - \{4\alpha(\varphi)\mathcal{A}^4(\varphi)[X\partial_X L(X) - L(X)]\} \right|_{r=r_H} = 0. \quad (46)$$

In this way the governing equations (29)–(31) together with the above boundary conditions (43)–(46), complement a well-posed boundary value problem. Since the position of the event horizon (the left boundary of the integration interval) is not fixed, moreover it is unknown⁷ and there is no analytic way to determine it, we can use one of

⁷Such BVPs are known in mathematical physics as BVPs of the Stefan kind.

these boundary conditions to determine it. We can introduce a new shifted independent variable $x = r - r_H$. In this way the domain of integration is completely defined – $x \in [0, \infty)$ and the radius of the horizon will appear explicitly in the equations as an unknown parameter. So, we have one parametric problem, which can be considered as a spectral-like nonlinear BVP.

Let us emphasize that there is an alternative formulation of the problem where the horizon is an input parameter. In this case we do not need a shifting map and the mass M becomes the sought parameter. We used this method of solution for justification of our results.

3.6 Method of solution

The system of ordinary differential equations (29)–(31) is coupled and nonlinear. It does not admit a global analytic solution and only some local expansions are possible. This is the reason to solve it numerically by using the reliable Continuous Analog of Newton’s Method, which is distinguished by its quadratic convergence in the vicinity of a localized root [62, 63]⁸. Yet, the method has been already successfully applied to similar problems (see, for example, [64, 38, 39, 46]).

4 Discussion of numerical results

As we noted in the previous sections we will consider constant parameter $\alpha > 0$ (α is defined by equation (12)). The results do not change qualitatively for different $\alpha > 0$ and we will present the results for $\alpha = 0.01$.⁹

In Figs. 1 and 2 the metric functions $m(r)$ and $\delta(r)$ and the scalar field $\varphi(r)$ for $P = 0.07$, $b = 10$, $\alpha = 0.01$ and for several values of the black hole mass are presented. An important justification of our results is that, up to the leading terms, the asymptotic form of the numerically obtained functions $\delta(r)$, $m(r)$, and $\varphi(r)$ at infinity is the same as what is predicted in (33), (34) and (35), respectively.

In Fig. 3 the horizon r_H and the temperature T as functions of the mass M for sequences of black hole solutions are plotted for $b = 10$ and $\alpha = 0.01$. Fig. 4 represents two magnifications of the enclosed regions on the $T(M)$ plot in Fig. 3. In Fig. 5 the value of the scalar field on the event horizon φ_H and the constant C_3 which occurs in the asymptotic expansion of the function $\varphi(r)$ at infinity (see equation (35)) as functions of the mass are plotted. In Figs. 6 and 7 the quantities r_H , T , φ_H and C_3 as functions of the charge P are plotted.

When $bP^2 > 1/8$ extremal black hole solutions exist in Einstein-Born-Infeld theory in AdS spacetime. In the presence of scalar field extremal black holes cannot exist as we have already proved. As we see from the $T(M)$ plot for $P = 0.113$ and $b = 10$ (this combination satisfies $bP^2 > 1/8$) in the right panel of Fig. 3, when M decreases the temperature first reaches values close to zero and afterward increases. The reason is that the absolute value of the scalar field rises considerably in this region, as we can

⁸Let us note that in our case the roots appear to be functions in Banach space.

⁹This value is consistent with the current observational data [45].

see in Fig. 5, and prevents the reaching of an extremal black hole. The same situation can be seen from the plot $T(P)$ in Fig. 6 when we increase the magnetic charge P (see, for example, the curve corresponding to $M = 0.10$).

The numerical results are obviously subject to and possess the properties in Subsection 3.3. All of the dependences have similar qualitative behavior in the parameter space that we have studied. The only exception is the function $T(M)$ because its qualitative behavior depends also on the value of the parameter b (more details on this subject will be given in the next sections).

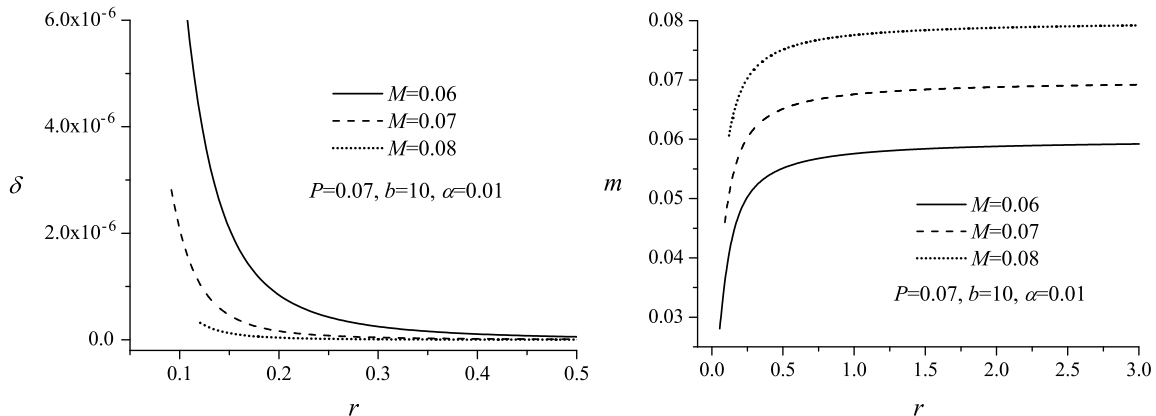


Figure 1: The metric functions $\delta(r)$ (left panel) and $m(r)$ (right panel) for several values of the black hole mass and for $P = 0.07$, $b = 10$, and $\alpha = 0.01$.

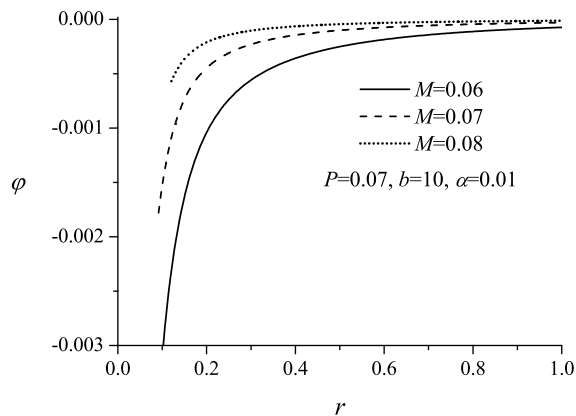


Figure 2: The scalar field $\varphi(r)$ for the same values of the parameters as in Fig. 1.

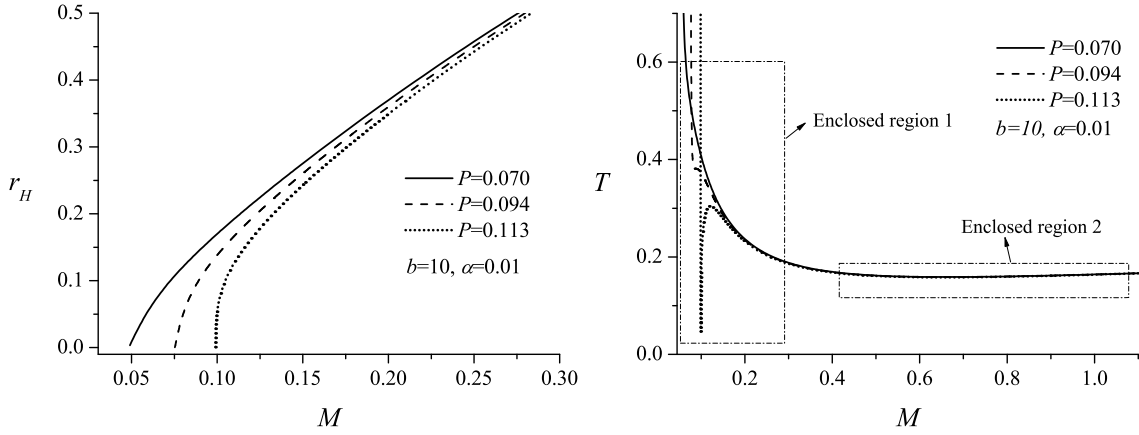


Figure 3: The radius of the black hole horizon r_H (left panel) and the temperature T (right panel) as functions of the mass M for sequences of black hole solutions ($b = 10$ and $\alpha = 0.01$). Note that on the right panel we denoted “Enclosed region 1” and “Enclosed region 2” which are expanded in Fig. 4.

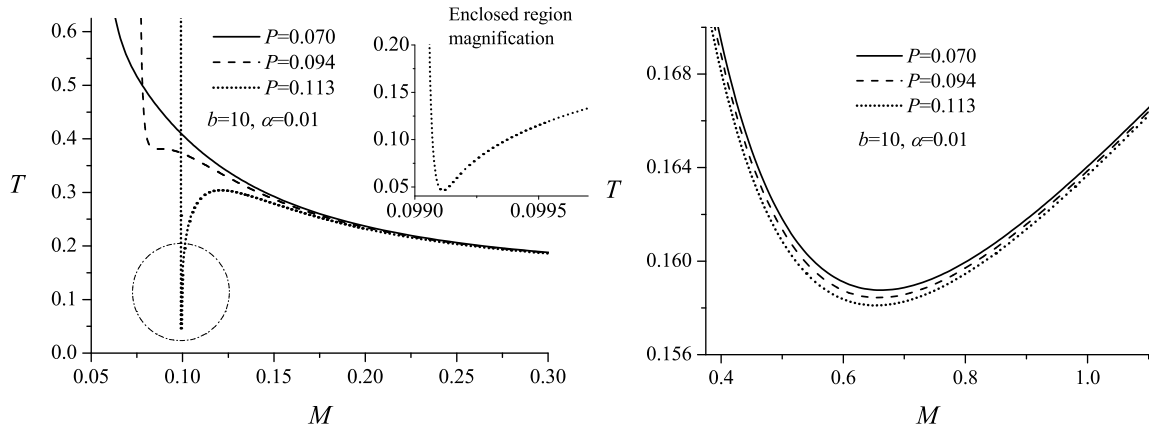


Figure 4: Magnifications of “Enclosed region 1” (left panel) and “Enclosed region 2” (right panel) of the $T(M)$ plot in Fig. 3.

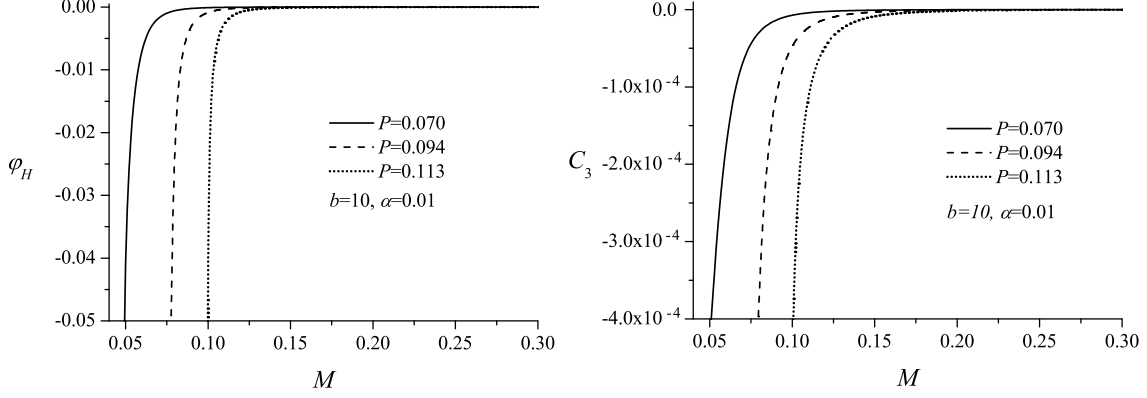


Figure 5: The scalar field on the horizon φ_H (left panel) and the constant C_3 (right panel) in the asymptotic expansion of the function $\varphi(r)$ at infinity (see equation (35)), as functions of the mass M for sequences of black hole solutions ($b = 10$ and $\alpha = 0.01$).

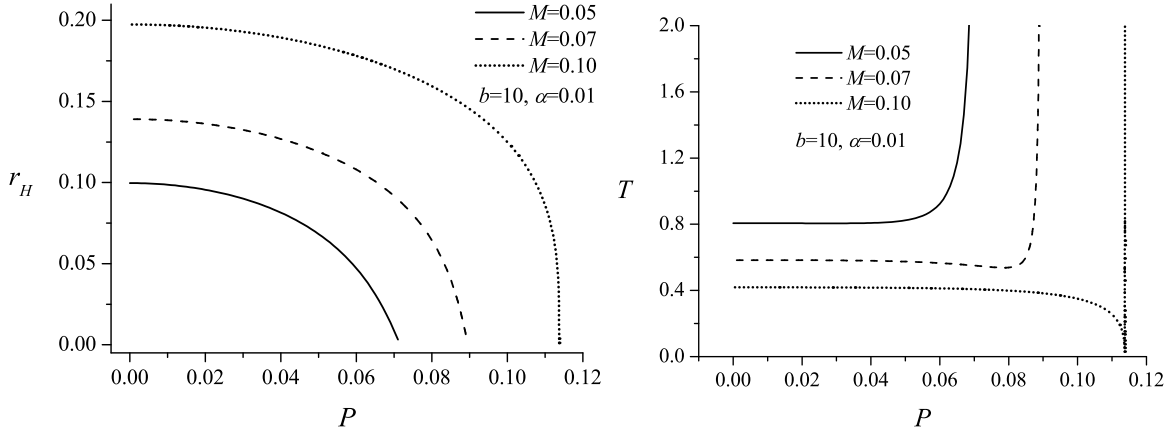


Figure 6: The radius of the black hole horizon r_H (left panel) and the temperature T (right panel) as functions of the charge P for sequences of black hole solutions ($b = 10$ and $\alpha = 0.01$).

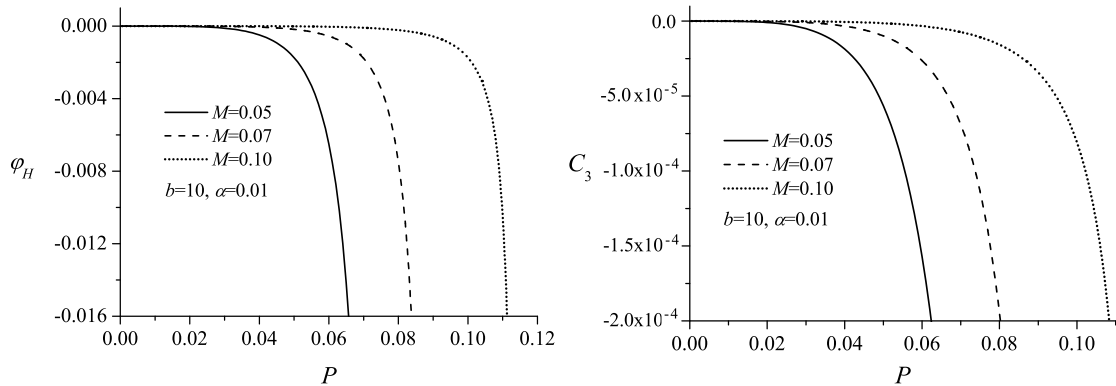


Figure 7: The scalar field on the horizon φ_H (left panel) and the constant C_3 (right panel) in the asymptotic expansion of the function $\varphi(r)$ at infinity (see equation (35)), as functions of the charge P for sequences of black hole solutions ($b = 10$ and $\alpha = 0.01$).

5 Thermodynamic phase structure

To study the thermodynamics¹⁰ of the black holes under consideration we need to find the conserved charges of our system first. Throughout the years many methods have been developed to calculate the conserved charges of the gravitational configurations. A related problem is the computation of the gravitational action of a noncompact spacetime. When evaluated on noncompact solutions, the bulk Einstein term and the boundary Gibbons-Hawking term are both divergent. The remedy is to consider these quantities relative to those associated with some background reference spacetime, whose boundary at infinity has the same induced metric as that of the original spacetime. This subtraction procedure is however connected to difficulties: the choice of the reference background is by no means unique and it is not always possible to embed a boundary with a given induced metric into the reference background. A new method, free of the aforementioned difficulties, was proposed in [65]. This method (called the counterterm method) consists of adding a (counter)term to the boundary at infinity, which is a functional only of the curvature invariants of the induced metric on the boundary. Unlike the subtraction procedure, this method is intrinsic to the spacetime of interest and is unambiguous once the counterterm which cancels the divergences is specified. In the present work we use, namely, the counterterm method in order to compute the mass and gravitational action. The technical details are presented in Appendix B.

We will study the thermodynamic phase structure for black holes in the canonical ensemble where the magnetic charge P is fixed. The associated thermodynamical potential in the case of the canonical ensemble, as one should expect from pure thermodynamical considerations, is the Helmholtz free energy $F(T, P) = M - TS$. This can be proven with more rigor by calculating the Euclidean action as it is done in Appendix B.

Let us note that our definition of the free energy is intrinsic. Our computation based on the counterterm method makes no reference to any other solution of the field equations. This should be contrasted with the method used in [47] where the authors compute the action using the extremal solution (with fixed charge) as reference background. As we already showed in our case there are no extremal solutions and therefore the reference background method of [47] is unapplicable.

The thermodynamic phase structure depends on the value of magnetic charge P and the parameter b in the Born-Infeld Lagrangian. The numerical results show that for large values of the parameter b the function $T = T(r_H, P)$ has two inflection points defined by

$$\frac{\partial T}{\partial r_H} = \frac{\partial^2 T}{\partial r_H^2} = 0. \quad (47)$$

These inflection points, which we will denote by $P_{\text{crit}}^{(1)}$ and $P_{\text{crit}}^{(2)}$, separate three charge intervals given by $P < P_{\text{crit}}^{(1)}$, $P_{\text{crit}}^{(1)} < P < P_{\text{crit}}^{(2)}$ and $P_{\text{crit}}^{(2)} < P$. Below we will consider each of these intervals in detail.

¹⁰Some clarifying comments on the black hole thermodynamics in scalar-tensor theories are given in Appendix A.

For small values of the parameter b the inflection points disappear and the phase structure is the same for all the charges. The numerical results show that for all of the studied values of the parameter α (including the case $\alpha = 0$ which corresponds to pure Einstein gravity) the critical value of the parameter b which separates the regions of small and large b , is $b_{\text{crit}} \approx 0.6$.

5.1 Phase structure for large values of the parameter $b > b_{\text{crit}}$

As we noted for large values of the parameter $b > b_{\text{crit}}$ the function $T = T(r_H, P)$ has two inflection points – $P_{\text{crit}}^{(1)}$ and $P_{\text{crit}}^{(2)}$, which gives us three charge intervals defined by $P < P_{\text{crit}}^{(1)}$, $P_{\text{crit}}^{(1)} < P < P_{\text{crit}}^{(2)}$ and $P_{\text{crit}}^{(2)} < P$. Formally we call these three cases black hole with small, intermediate and large charge respectively. On its own side the intermediate charge interval has to be divided into three subintervals $P_{\text{crit}}^{(1)} < P < P_{\text{ph}}^{(1)}$, $P_{\text{ph}}^{(1)} < P < P_{\text{ph}}^{(2)}$ and $P_{\text{ph}}^{(2)} < P < P_{\text{crit}}^{(2)}$ ($P_{\text{ph}}^{(1)}$ and $P_{\text{ph}}^{(2)}$ are defined and discussed in details in the following subsections). As we show below, there are phase transitions for charges belonging to the second and the third subintervals.

All the results for the scalar-tensor black holes given in this subsection are computed for fixed values of the parameters $b = 10$ and $\alpha = 0.01$. For this choice of parameters the values of the critical charges are $P_{\text{crit}}^{(1)} = 0.09397$ and $P_{\text{crit}}^{(2)} = 0.2901$. The value of $P_{\text{crit}}^{(2)}$ is the same (within the numerical error) as in the pure Einstein theory (i.e. for $\alpha = 0$). The reason is that the corresponding inflection point, defined by equation (47), is situated in a region of the parameter space where the contribution of the scalar field is very small. The value of $P_{\text{crit}}^{(1)}$ in the case of pure Einstein theory – $P_{\text{crit}}^{(1)} \alpha=0 = 0.09395$, is a bit smaller than in the case when scalar field is present. The numerical results for larger α confirm that $P_{\text{crit}}^{(1)}$ increases slightly when we increase the value of the coupling constant α .

The values of the charges $P_{\text{ph}}^{(1)}$ and $P_{\text{ph}}^{(2)}$ for the chosen values of the parameters $b = 10$ and $\alpha = 0.01$, are $P_{\text{ph}}^{(1)} = 0.1087$ and $P_{\text{ph}}^{(2)} = 0.1093$ and the corresponding values in pure Einstein theory are $P_{\text{ph}}^{(1)} \alpha=0 = 0.1085$ and $P_{\text{ph}}^{(2)} \alpha=0 = 0.1091$. The numerical experiments show that the values of $P_{\text{ph}}^{(1)}$ and $P_{\text{ph}}^{(2)}$ increase slightly with the increase of α .

The temperature T as a function of the horizon radius r_H is shown in Fig. 8 for the cases of small (for example $P=0.07$), intermediate (for example $P=0.115$), and large (for example $P=0.40$) charges P . The free energy F as a function of the temperature T for small and intermediate charges is shown in Fig. 9 and magnifications of specific regions are presented in Fig. 10. The function $F(T)$ for various charges, including large charges, is given in the left panel of Fig. 12. In Figs. 11 and 12 (right panel) we also give the dependences $T(r_H)$ and $F(T)$ for Born-Infeld-AdS (BIAdS) black holes in the pure Einstein gravity for comparison. The figures show that the thermodynamic phase structures for the scalar-tensor BIAdS black holes and the Einstein BIAdS black holes are qualitatively the same except in the case of charges satisfying $bP^2 > 1/8$ where additional phases of the scalar-tensor BIAdS black holes are present. Below we consider in detail the thermodynamic phase structure for the intervals of small, intermediate and large charges.

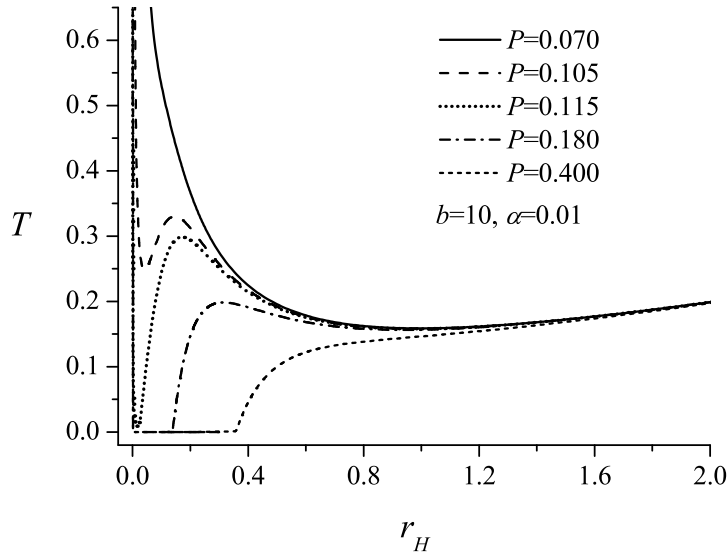


Figure 8: The temperature T as a function of the radius of the horizon r_H for sequences of black hole solutions ($b = 10$ and $\alpha = 0.01$).

The phase structure and the phase transitions can be alternatively studied with the so-called off-shell formalism or, in other words, off-equilibrium formalism. It is thoroughly presented in [66] and applied, for example, in the papers on black-hole phase transitions by Myung and coauthors [50, 51, 47]. The advantage of that formalism is that it gives a simple and clear interpretation of the thermodynamic phases. In the canonical ensemble the different phases of the system, both stable and unstable, correspond to extrema of the so-called off-shell free energy. In that formalism, the origin of the branches in the $T - F$ diagram, that correspond to the different phases, can be also simply explained. The phase transitions have been studied with the application of the off-shell formalism in Appendix C.

5.1.1 Phase structure for small charges

In the region of small charges $P < P_{\text{crit}}^{(1)}$, as one can see from Fig. 13, for arbitrary temperature $T > T_0$ there are two branches of solutions for the black hole radius. These two branches correspond to small and large black holes, respectively. The small black holes have negative specific heat C_P which is defined according to the formula

$$C_P = T \left. \frac{\partial S}{\partial T} \right|_P = 2\pi T r_H \left. \left(\frac{\partial T}{\partial r_h} \right)^{-1} \right|_P \quad (48)$$

and therefore they are unstable. The large black holes have positive specific heat and consequently they are locally stable. Moreover, as can be seen in Fig. 13 (right panel) the free energy of the large black holes is smaller than the free energy of the small black holes and therefore the large black holes are thermodynamically favorable and dominate the thermodynamic ensemble.

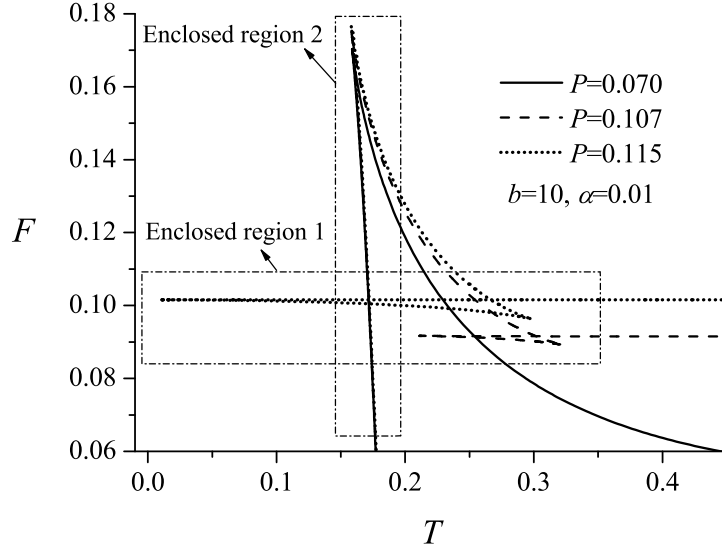


Figure 9: The free energy F as a function of the temperature T for sequences of black hole solutions ($b = 10$ and $\alpha = 0.01$). Note that in the figure we defined “Enclosed region 1” and “Enclosed region 2” which are expanded in Fig. 10

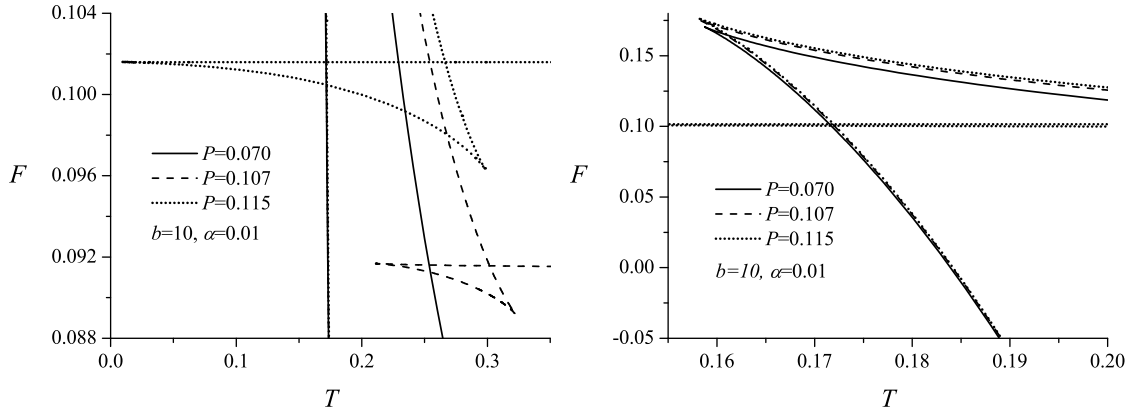


Figure 10: Magnifications of the enclosed regions of the $F(T)$ plot in Fig. 9. The left panel corresponds to “Enclosed region 1” and the right panel corresponds to “Enclosed region 2”.

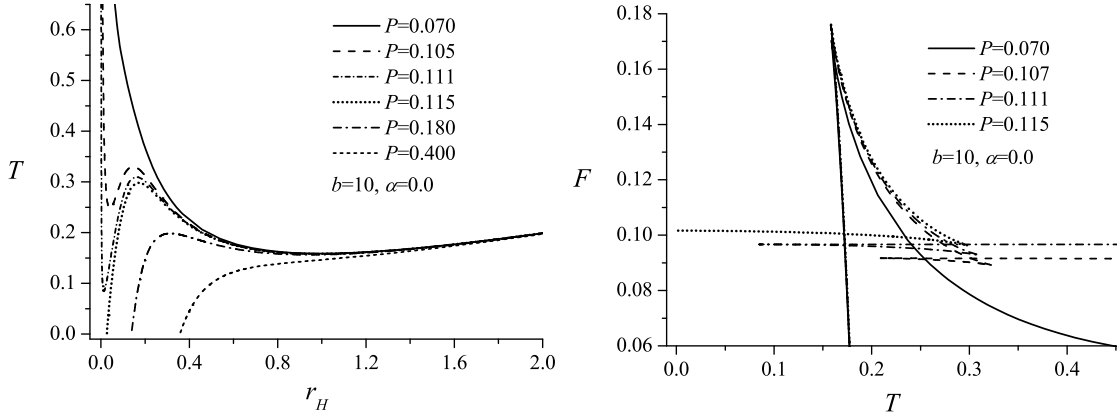


Figure 11: The functions $T(r_H)$ and $F(T)$ for sequences of black hole solutions in pure Einstein theory ($b = 10$ and $\alpha = 0.0$).

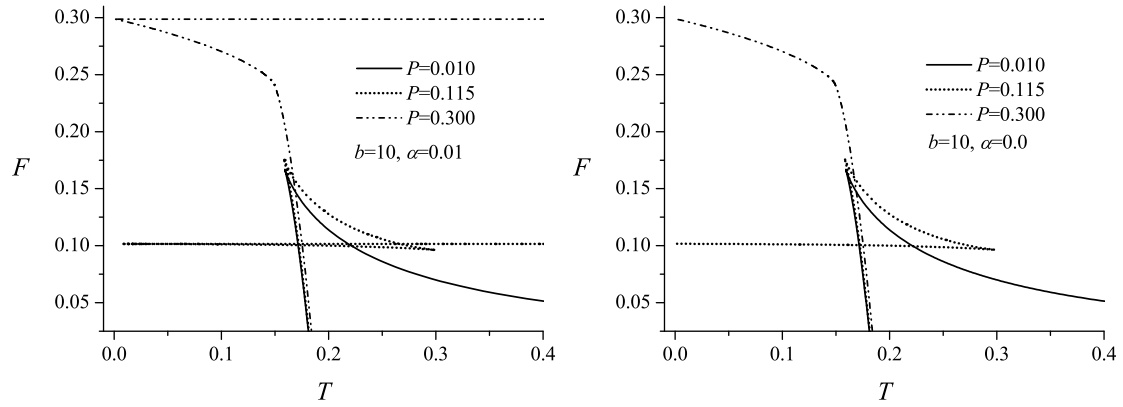


Figure 12: The function $F(T)$ for sequences of black hole solutions with various charges P , including large charges, in the case when $\alpha = 0.01$ (left panel) and for pure Einstein theory – $\alpha = 0.0$ (right panel).

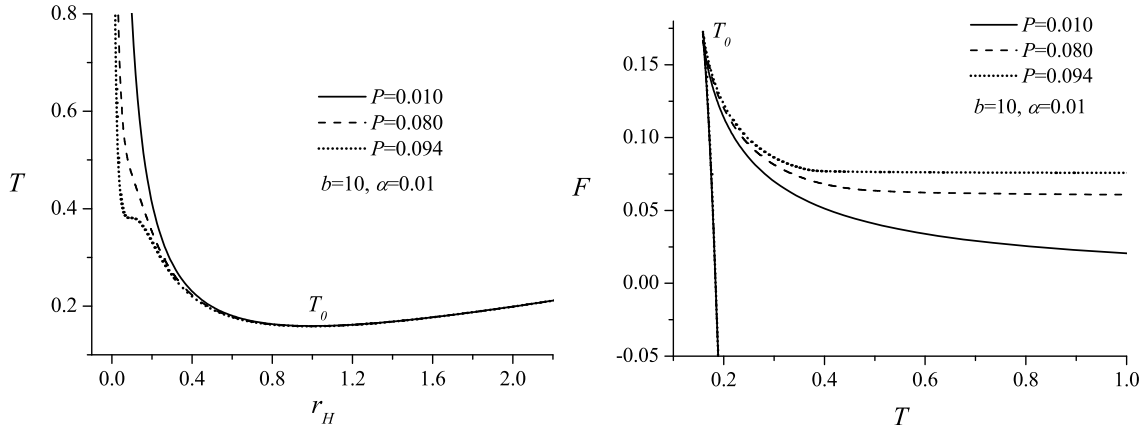


Figure 13: The functions $T(r_H)$ and $F(T)$ for small charges where $b = 10$ and $\alpha = 0.01$. The curve corresponding to the critical charge $P_{\text{crit}}^{(1)}$ is denoted by the dotted line.

5.1.2 Phase structure for intermediate charges

In the intermediate charge interval defined by $P_{\text{crit}}^{(1)} < P < P_{\text{crit}}^{(2)}$, there are four branches, as shown in Figs. 14–17. These branches will be called branches of very small (VSBH), small (SBH), large (LBH), and very large (VLBH) black holes, respectively.

Below we describe the phase structure in the subintervals $P_{\text{crit}}^{(1)} < P < P_{\text{ph}}^{(1)}$, $P_{\text{ph}}^{(1)} < P < P_{\text{ph}}^{(2)}$ and $P_{\text{ph}}^{(2)} < P < P_{\text{crit}}^{(2)}$. The differences between the three subintervals are that in the first subinterval no phase transitions exist, in the second subinterval phase transitions of first and zeroth order exist, and in the third subinterval only first order phase transition exists. Such subintervals with the corresponding phase transitions are also present for pure Einstein-Born-Infeld-AdS black holes.

Intermediate charge subinterval $P_{\text{crit}}^{(1)} < P < P_{\text{ph}}^{(1)}$

In this subinterval $T_0 < T_{\text{min}}$ ¹¹. The $T(r_H)$ and $F(T)$ dependences are shown in Figs. 14 and 15 and the phase structure is described as follows. For low temperature T satisfying $T_0 < T < T_{\text{min}}$ there are two solutions for the black hole horizon radius corresponding to LBH and VLBH. From the dependence $T(r_H)$ shown in Fig. 14 one can conclude that the LBH are thermodynamically unstable since they have negative specific heat, while the VLBH have positive specific heat and therefore they are locally stable. At $T = T_{\text{min}}$ the origin of two new branches of solutions appears and for $T_{\text{min}} < T < T_{\text{max}}$ we have four black holes with the same temperature and different radii – VSBH, SBH, LBH, and VLBH. The VSBH and LBH are unstable since their specific heat is negative, while the SBH and VLBH have positive specific heat and consequently they are locally stable. At $T = T_{\text{max}}$ two of the branches coalesce and disappear, leaving only two branches for $T > T_{\text{max}}$ corresponding to unstable VSBH

¹¹By T_0 and T_{min} we denote the two minima of the $T(r_H)$ function as can be seen in Fig. 14.

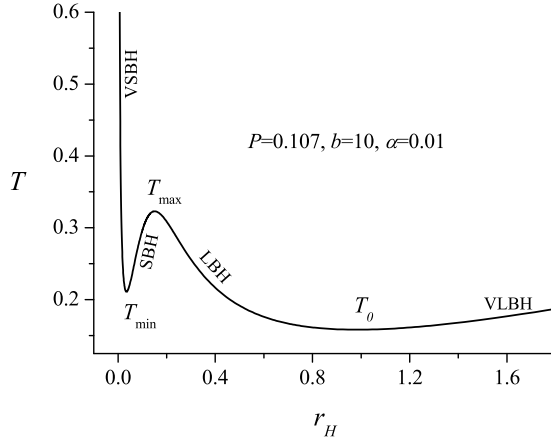


Figure 14: The function $T(r_H)$ for intermediate charge $P_{\text{crit}}^{(1)} < P < P_{\text{ph}}^{(1)}$ ($P = 0.107$, $b = 10$ and $\alpha = 0.01$).

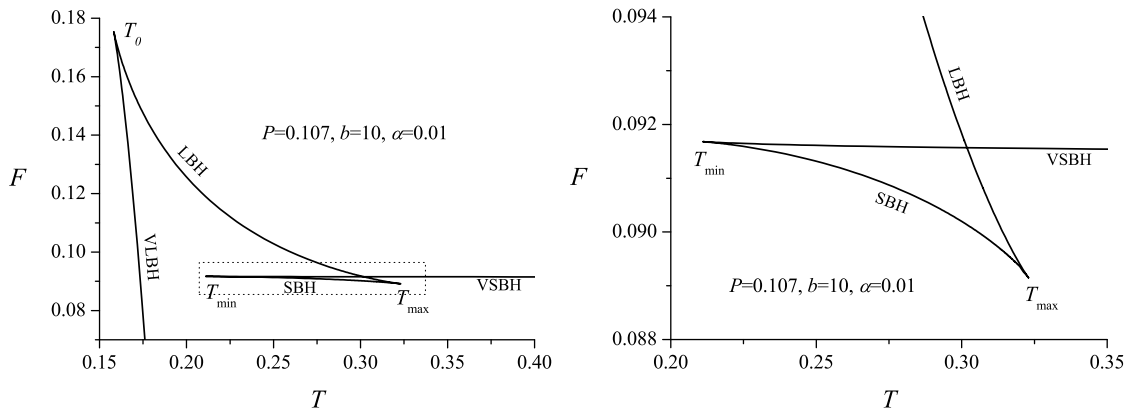


Figure 15: The function $F(T)$ for intermediate charge $P_{\text{crit}}^{(1)} < P < P_{\text{ph}}^{(1)}$ ($P = 0.107$, $b = 10$ and $\alpha = 0.01$). The right panel is a magnification of the enclosed region of the left figure.

and locally stable VLBH. From $T = T_0$ to arbitrary large temperature the free energy of the VLBH, corresponding to the leftmost branch in Fig. 15 (left panel) (corresponding to the rightmost branch in Fig. 14), is the smallest which means that for arbitrary temperature the VLBH dominate the thermodynamic ensemble.

Intermediate charge subinterval $P_{\text{ph}}^{(1)} < P < P_{\text{ph}}^{(2)}$

In this subinterval $T_0 < T_{\text{min}}$. The $T(r_H)$ and $F(T)$ dependences are shown in Fig. 16 and the phase structure is described as follows. For $T_0 < T < T_{\text{min}}$ we have two branches – unstable LBH and locally stable VLBH. At $T = T_{\text{min}}$ two new branches appear and for $T_{\text{min}} < T < T_{\text{max}}$ there are four branches corresponding to unstable VSBH, locally stable SBH, unstable LBH and locally stable VLBH. At T_{max} two of the branches coalesce and disappear and we are left with only two branches of unstable VSBH and locally stable VLBH. From T_0 to T_{min} the VLBH have the smallest free

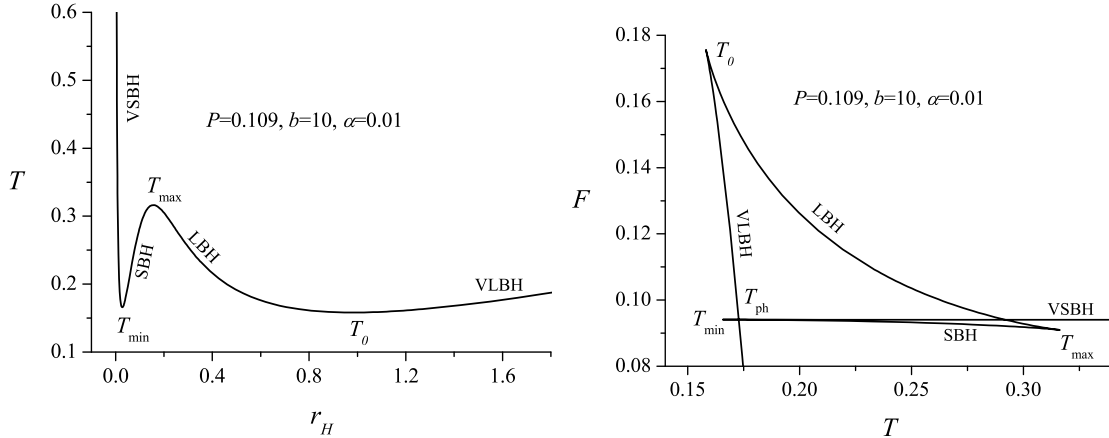


Figure 16: The functions $T(r_H)$ and $F(T)$ for intermediate charges $P_{\text{ph}}^{(1)} < P < P_{\text{ph}}^{(2)}$ ($P = 0.109$, $b = 10$ and $\alpha = 0.01$).

energy and they dominate the thermodynamical ensemble. At $T = T_{\text{min}}$ the situation changes and for temperatures in the interval from T_{min} to T_{ph} the ensemble is dominated by the SBH which have the smallest free energy. At this point $T = T_{\text{min}}$ phase transition between VLBH and SBH occurs and it is zeroth order phase transition since the free energy is discontinuous at that point – the free energy jumps to a lower value¹². Such unusual phase transitions of zeroth order have been observed for example in [67, 68, 69].

As we said for temperatures in the interval $T_{\text{min}} < T < T_{\text{ph}}$ the ensemble is dominated by the SBH. As we can see in Fig. 16 for arbitrary $T > T_{\text{ph}}$ the ensemble is again dominated by the VLBH which have the smallest free energy. This means that at the point $T = T_{\text{ph}}$ we observe a phase transition between the SBH and VLBH and it is classified as a first order phase transition since the free energy is continuous at $T = T_{\text{ph}}$ and the first derivative of the free energy is discontinuous at that point.

Intermediate charge subinterval $P_{\text{ph}}^{(2)} < P < P_{\text{crit}}^{(2)}$

In this subinterval $T_{\text{min}} < T_0$. The $T(r_H)$ and $F(T)$ dependences are shown in Fig. 17 and the phase structure is described as follows. For $T_{\text{min}} < T < T_0$ there are two branches corresponding to unstable VSBH and locally stable SBH. At $T = T_0$ two new branches appear and for temperatures $T_0 < T < T_{\text{max}}$ we have four branches corresponding to unstable VSBH, locally stable SBH, unstable LBH and locally stable VLBH. At $T = T_{\text{max}}$ the branches of SBH and LBH disappear and we are left with unstable VSBH and locally stable VLBH for $T > T_{\text{max}}$. From T_{min} to temperature T_{ph} the free energy of the SBH is the smallest and the SBH dominate the thermodynamic ensemble. At temperature $T = T_{\text{ph}}$ the free energy of the VLBH becomes smaller than the free energy of the SBH and for all temperatures $T > T_{\text{ph}}$ the VLBH dominate the thermodynamic ensemble. At the point $T = T_{\text{ph}}$ we have a first-order phase transition from SBH to VLBH.

¹²We have studied the zeroth-order phase transition observed at that point with the off-shell formalism in Appendix C.

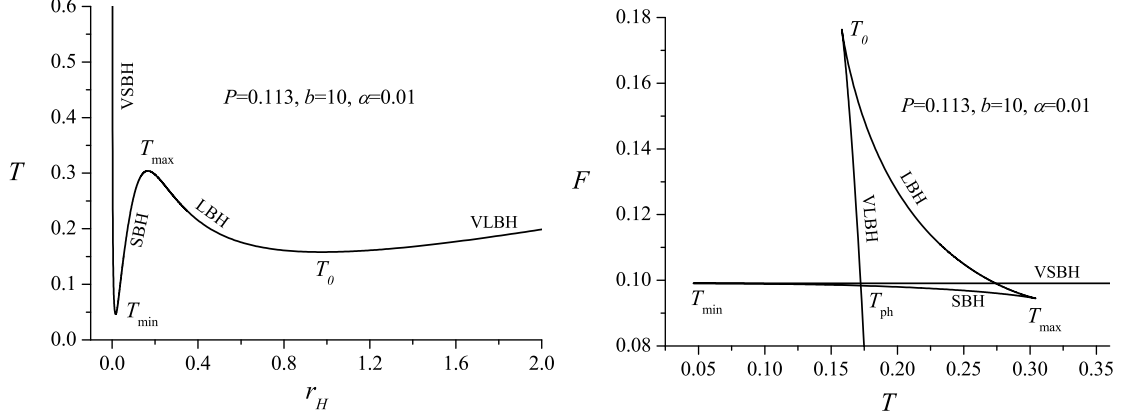


Figure 17: The functions $T(r_H)$ and $F(T)$ for intermediate charge $P_{\text{ph}}^{(2)} < P < P_{\text{crit}}^{(2)}$ ($P = 0.113$, $b = 10$ and $\alpha = 0.01$).

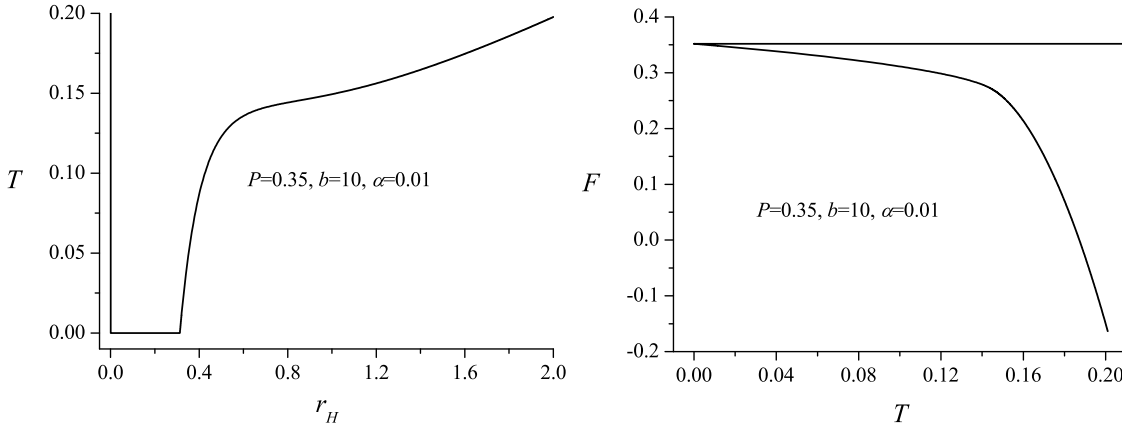


Figure 18: The functions $T(r_H)$ and $F(T)$ for large charge $P_{\text{crit}}^{(2)} < P$ ($P = 0.35$, $b = 10$ and $\alpha = 0.01$).

5.1.3 Phase structure for large charges

In the case of large charges defined by $P_{\text{crit}}^{(2)} < P$, there are two branches – small and large black holes, as Fig. 18 shows. The small black holes have negative specific heat and consequently they are unstable. The large black holes are locally stable since their specific heat is positive. For arbitrary temperature the free energy of the large black holes is smaller than the free energy of the small black holes. Therefore the large black holes dominate the thermodynamic ensemble.

5.2 Phase structure for small values of the parameter $b < b_{\text{crit}}$

The phase structure for small values of the parameter b is much simpler because the function $T = T(r_H, P)$ has no inflection point. Therefore the phase structure is qualitatively the same for all values of the magnetic charge P . The functions $T(r_H)$ and $F(T)$ are plotted in Fig. 19 for $b = 0.1$ and $\alpha = 0.01$. Only two branches exist corresponding to unstable small black holes and locally stable large black hole. The large black holes

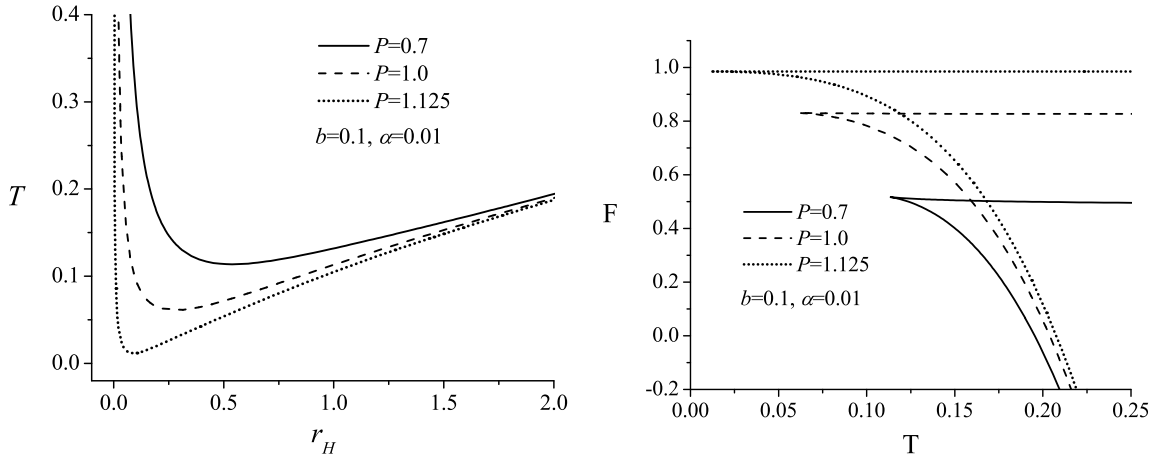


Figure 19: The functions $T(r_H)$ and $F(T)$ for a small value of the Born-Infeld parameter $b = 0.1$ ($\alpha = 0.01$).

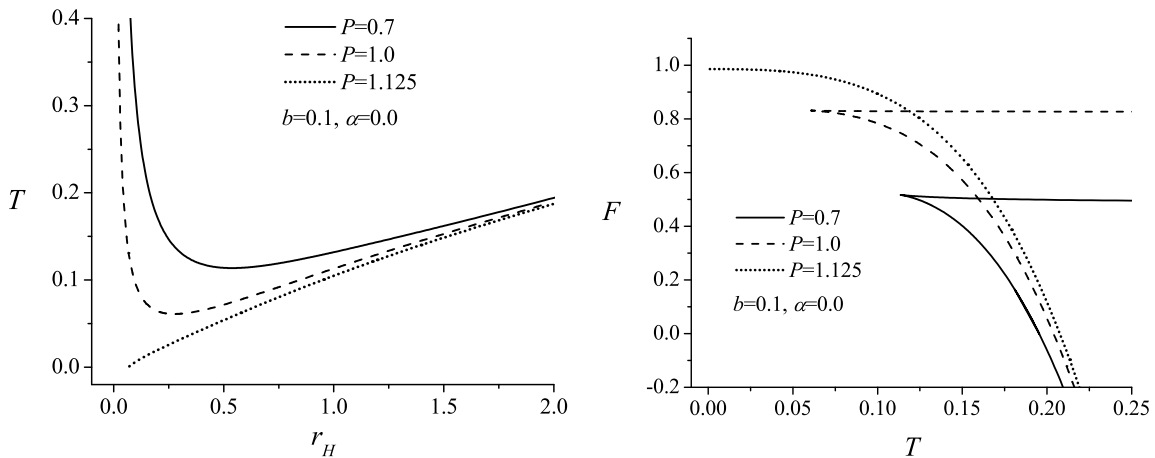


Figure 20: The functions $T(r_H)$ and $F(T)$ for sequences of black hole solutions in pure Einstein gravity ($\alpha = 0.0$) for a small value of the Born-Infeld parameter $b = 0.1$.

have lower free energy and therefore they dominate the thermodynamic ensemble.

The functions $T(r_H)$ and $F(T)$ for $b = 0.1$ are shown in Fig. 20 in the case of pure Einstein theory which corresponds to $\alpha = 0.0$. This case is qualitatively the same as the case when the scalar field is nontrivial except for large charges which fulfill the inequality $bP^2 > 1/8$. For these values of b and P , when $\alpha = 0.0$, the branch of small black holes disappear because of the occurrence of an extremal black hole (see for example the curve corresponding to $P = 1.125$ in Fig. 20).

6 Conclusion

In the current paper we have constructed numerically new scalar-tensor black hole solutions in AdS space-time coupled to Born-Infeld nonlinear electrodynamics. The properties of the solutions have been thoroughly studied through a combination of

analytical and numerical techniques. The black hole solutions in the considered class of scalar-tensor theories are determined uniquely by the asymptotic charges of the black holes – in our case the mass and the magnetic charge. An important property is that in comparison to the corresponding solutions in General Relativity, namely, the Einstein-Born-Infeld-AdS black holes, the black holes considered here have a simpler causal structure – they have neither inner nor degenerate horizons.

The thermodynamics and the phase structure in the canonical ensemble of the obtained black holes have also been studied. Their phase structure is similar to that of the Einstein-Born-Infeld-AdS black holes in GR and the difference is manifested at large charges. This means that in the case under consideration there are no extremal black hole solutions which actually leads to one additional branch of solutions in the thermodynamical phase-space structure for large values of the charge.

The thermodynamical phase-space structure depends on the Born-Infeld parameter b and the magnetic charge P . A critical value $b_{\text{crit}} \approx 0.6$ has been found numerically. For $b < b_{\text{crit}}$ the phase diagram is the same for all values of the magnetic charge P . There are two branches corresponding to unstable, small black holes and locally stable, large black holes. In this case no phase transitions are possible.

In the case of $b > b_{\text{crit}}$, the structure of the phase diagram changes with the variation of the magnetic charge P and three charge intervals are observed – small, intermediate, and large charges. For small and large values of the magnetic charge no phase transitions are possible and the phase diagram has only two branches which corresponds to two phases: unstable, small black holes and locally stable, large black holes. The intermediate charges are the most interesting because phase transitions can exist in this case. The phases are four: VSBH, SBH, LBH, and VLBH. Among them two are locally stable – the SBH and the VLBH – and phase transitions between the two black holes are possible in some cases. In the intermediate charge subinterval $P_{\text{ph}}^{(2)} < P < P_{\text{crit}}^{(2)}$ first order phase transition between SBH and VLBH exists – for small values of the temperature ($T_0 < T < T_{\text{ph}}$) the SBH are thermodynamically favorable because they have lower free energy. When we increase the temperature we reach a certain value of the temperature T_{ph} where phase transition to VLBH occurs and for all temperatures above that value $T > T_{\text{ph}}$ the VLBH are thermodynamically favorable. This phase transition is of first order because the first derivative of the free energy is discontinuous at that point. An important observation is that for a small intermediate charge subinterval $P_{\text{ph}}^{(1)} < P < P_{\text{ph}}^{(2)}$ two phase transitions exist. One of them is the first order phase transition we just described and the other one is the zeroth order phase transition. In this case for small values of the temperature ($T_0 < T < T_{\text{min}}$) the only locally stable branch is the VLBH. At temperature T_{min} another locally stable branch appears – SBH, which have the smallest free energy and dominate the thermodynamical ensemble. This means that for $T = T_{\text{min}}$ phase transition between VLBH and SBH exists and it is of zeroth order since the free energy is discontinuous at that point. When we increase the temperature the point $T = T_{\text{ph}}$ is reached where the first order phase transition between SBH and VLBH, that was described above, occurs. For $T > T_{\text{ph}}$ again the VLBH dominate the thermodynamical ensemble. For all the other intermediate charges phase transitions are not possible since the free energy of the VLBH is always the smallest. Similar zeroth and first order phase transitions for certain charge

intervals are present also in the corresponding solutions in General Relativity.

Let us finish with prospects for future work. As in the asymptotically flat case [46], in AdS spacetimes the scalar-tensor theories with $\alpha(\varphi) = \beta\varphi$ ($\beta < 0$) coupled to nonlinear electrodynamics admit non-unique black hole solutions [70]. From AdS/CFT perspectives these non-unique black hole solutions could be considered as second order phase transitions in the dual field theory living on the boundary. Detailed considerations will be given in a forthcoming paper [70]. Phase transitions due to non-unique AdS black hole solutions in Einstein-Maxwell-dilaton gravity with appropriate dilaton coupling function have been obtained quite recently in [71]. Let us note however that the situation in the case of scalar-tensor AdS black holes coupled to the nonlinear electrodynamics is rather different in comparison with the Einstein-Maxwell-dilaton gravity.

Acknowledgements

S.Y. would like to thank D. Uzunov for the discussions on phase transitions. D.D. would like to thank the DAAD for a scholarship and the Institute for Astronomy and Astrophysics Tübingen for its kind hospitality. D.D. would also like to thank J. Kunz, B. Kleihaus, and D. Georgieva for the helpful discussions.

This work was partially supported by the Bulgarian National Science Fund under Grants DO 02-257, VUF-201/06, and by Sofia University Research Fund under Grant No 074/2009.

A Black hole thermodynamics in scalar-tensor theories

In this appendix we would like to make some comments on the thermodynamics of the black holes in scalar-tensor theories. The definitions of entropy, temperature, and mass (energy) of the scalar-tensor black hole are naturally related to the Einstein frame. The reasons are the following. The Einstein-frame area of the horizon can be interpreted as entropy of the horizon since it is non-decreasing in classical physical processes. The entropy of the event horizon in the Einstein frame S_E , for example, is proportional to one fourth of the area of the horizon. In the Jordan frame, however, the area of the event horizon may decrease in classical processes [72] and a generalized definition of entropy S_J needs to be introduced. The proper definition is [72, 73, 74, 75]

$$S_J = \frac{1}{4G_*} \int d^2x \sqrt{-^{(2)}\tilde{g}} F(\Phi). \quad (49)$$

This definition is also consistent with the Euclidean and the Noether charge method [74].

Using relation (2) we find that

$$S_J = \frac{1}{4G_*} \int d^2x \sqrt{-^{(2)}g} = S_E = S, \quad (50)$$

the definitions of the entropy in both conformal frames are in agreement. In the last two equations quantities ${}^{(2)}\tilde{g}$ and ${}^{(2)}g$ are the determinants of the induced metrics on the horizon in the Jordan and in the Einstein frames, respectively.

Further, it can be proved that the standard definitions of black-hole temperature are invariant with respect to conformal transformations that are regular on the event horizon [76]. Since the conformal transformations (2) in the present paper are regular on the horizon (and everywhere outside the horizon), the temperature in the Einstein frame coincides with the temperature in the Jordan frame.

The measure of the internal energy of compact objects in STT needs also to be specified. In the general case the masses of the black holes in the Einstein frame and in the Jordan frame do not coincide. The mass in the Einstein frame is positive definite, can only decrease by emission of gravitational (and scalar waves), and possesses other natural energy-like properties unlike the mass in the Jordan frame. In other words the mass in the Einstein frame is the true energy of the compact objects within the framework of the STT. For more details on the mass of compact objects in the STT we refer the reader to [77, 78, 79, 80, 38, 39]. For the particular solutions studied in the current paper, however, the scalar field decreases fast enough and the black-hole masses in both conformal frames are the same.

B Derivation of the free energy

The action with surface terms and counterterms taken into account is given by

$$S = \frac{1}{16\pi} \int_{\mathcal{M}} d^4x \sqrt{-g} \left(R - 2g^{\mu\nu} \partial_\mu \varphi \partial_\nu \varphi + \frac{6}{\ell^2} + 4\mathcal{A}^4(\varphi)L(X) \right) + \frac{1}{8\pi} \int_{\partial\mathcal{M}} d^3x \sqrt{-\gamma} \Theta[\gamma] - \frac{1}{8\pi} S_{\text{ct}}[\gamma] \quad (51)$$

where $\gamma_{\mu\nu}$ is the metric induced on the boundary $\partial\mathcal{M}$ and Θ is the trace of the extrinsic curvature of $\partial\mathcal{M}$ while $S_{\text{ct}}[\gamma]$ is the counterterm action. We have also defined $\ell = \sqrt{-3/\Lambda}$ and the boundary stress-energy tensor is given by

$$\mathcal{T}^{\mu\nu} = \frac{2}{\sqrt{-\gamma}} \frac{\delta S}{\delta \gamma_{\mu\nu}} = \frac{1}{8\pi} \left[\Theta^{\mu\nu} - \Theta \gamma^{\mu\nu} + \frac{2}{\sqrt{-\gamma}} \frac{\delta S_{\text{ct}}}{\delta \gamma_{\mu\nu}} \right]. \quad (52)$$

If the boundary geometry has an isometry generated by the Killing vector K , $\mathcal{T}_{\mu\nu} K^\nu$ is divergence free which gives the conserved quantity

$$\mathcal{Q}_K = \int_\sigma d\sigma^\mu \mathcal{T}_{\mu\nu} K^\nu \quad (53)$$

associated with the closed surface σ in the boundary $\partial\mathcal{M}$. In the case when $K = \partial/\partial t$, the conserved quantity is the mass.

For spacetimes with AdS asymptotic the following simple counterterm was proposed in [65] (see also [81])

$$S_{\text{ct}} = \int_{\partial\mathcal{M}} d^3x \sqrt{-\gamma} \frac{2}{\ell} \left(1 + \frac{\ell^2}{4} \mathcal{R}[\gamma] \right) \quad (54)$$

where $\mathcal{R}[\gamma]$ is the Ricci scalar curvature of the boundary metric $\gamma_{\mu\nu}$. With this counterterm for the asymptotic metric

$$ds^2 \approx - \left(1 - \frac{2M}{r} + \frac{r^2}{\ell^2} \right) dt^2 + \frac{dr^2}{1 - \frac{2M}{r} + \frac{r^2}{\ell^2}} + r^2 (d\theta^2 + \sin^2 \theta d\phi^2) \quad (55)$$

we have up to the leading order

$$8\pi\mathcal{T}_{tt} = \frac{2M}{r\ell} + \mathcal{O}(r^{-2}) \quad (56)$$

which gives the mass

$$\mathcal{Q}_\xi = M. \quad (57)$$

In other words this shows that the limit $\lim_{r \rightarrow \infty} m(r) = M$ of the metric function $m(r)$ (see eq.(28)) has to be identified with the mass of the solutions with AdS asymptotic.

Our next task is to calculate the Euclidean action. For definiteness we shall consider the electrically charged case. First to make the action Euclidean, the time coordinate should be made imaginary by substitute $t = i\tau$. This makes the metric positively definite, namely

$$ds^2 = f(r) e^{-2\delta(r)} d\tau^2 + \frac{dr^2}{f(r)} + r^2 (d\theta^2 + \sin^2 \theta d\phi^2). \quad (58)$$

In order to eliminate the conical singularity at the horizon $r = r_H$, the Euclidean time coordinate τ has to be periodic with period $\beta = 1/T$ where T is the Hawking temperature associated with the black hole horizon. The very Euclidean action is given by

$$I = I_{\text{bulk}} + I_\Theta + I_{\text{ct}} + I_{\text{cf}} \quad (59)$$

where

$$I_{\text{bulk}} = -\frac{1}{16\pi} \int_{\mathcal{M}} d^4x \sqrt{g} \left(R - 2g^{\mu\nu} \partial_\mu \varphi \partial_\nu \varphi + \frac{6}{\ell^2} + 4\mathcal{A}^4(\varphi)L(X) \right), \quad (60)$$

$$I_\Theta = -\frac{1}{8\pi} \int_{\partial\mathcal{M}} d^3x \sqrt{\gamma} \Theta[\gamma], \quad (61)$$

$$I_{\text{ct}} = \frac{1}{8\pi} \int_{\partial\mathcal{M}} d^3x \sqrt{\gamma} \frac{2}{\ell} \left(1 + \frac{\ell^2}{4} \mathcal{R}[\gamma] \right), \quad (62)$$

$$I_{\text{cf}} = \frac{1}{4\pi} \int_{\partial\mathcal{M}} d^3x \sqrt{\gamma} n_\mu A_\nu F^{\mu\nu} \mathcal{A}^4(\varphi) \partial_X L. \quad (63)$$

The bulk integral is on compact region \mathcal{M} with boundary $\partial\mathcal{M}$. The boundary $\partial\mathcal{M}$ lays at finite radius $r = r_B$ and has topology $S^1 \times S^2$ where S^1 stands for the periodic Euclidean time coordinate τ . The last term I_{cf} is a charge fixing term, in other words we have added this term since we consider a fixed charge ensemble.

In order to compute the Euclidean action and to show that $I/\beta = M - TS$ we will need an auxiliary tool, namely the Komar integral

$$\tilde{M}_B = -\frac{1}{8\pi} \int_{S_B^2} \nabla^\mu \xi^\nu dS_{\mu\nu} \quad (64)$$

where S_B^2 is a sphere with radius r_B and ξ is the timelike Killing vector. Obviously the Komar integral is divergent for $r_B \rightarrow \infty$ but it is finite for finite r_B . More precisely, for the AdS asymptotic (55) we have

$$\tilde{M}_B = M + \frac{r_B^3}{\ell^2} + \mathcal{O}\left(\frac{1}{r_B}\right). \quad (65)$$

Using Stokes theorem we can present the Komar integral as a sum of integral on the horizon \mathcal{H} and a bulk integral

$$\tilde{M}_B = -\frac{1}{8\pi} \int_{\mathcal{H}} \nabla^\mu \xi^\nu dS_{\mu\nu} - \frac{1}{4\pi} \int_{\Sigma} R_{\mu\nu} \xi^\nu d\Sigma^\mu \quad (66)$$

where Σ is the 3-dimensional space bounded by S_B^2 and \mathcal{H} .

It is well known that the integral on the horizon gives just

$$-\frac{1}{8\pi} \int_{\mathcal{H}} \nabla^\mu \xi^\nu dS_{\mu\nu} = 2TS \quad (67)$$

where T is the Hawking temperature and S is the black hole entropy which is one fourth of the horizon area. On the other hand using the field equations we find

$$R_{\mu\nu} \xi^\nu = \Lambda \xi_\mu - 2\partial_X L F_{\mu\alpha} F_\nu{}^\alpha \xi^\nu + 2\mathcal{A}^4(\varphi) [2X\partial_X L - L] \xi_\mu. \quad (68)$$

Now we introduce the electric potential Φ by the equation $\partial_\alpha \Phi = -\xi^\nu F_{\nu\alpha}$ and taking into account the field equations for the electromagnetic field, the second term on the right-hand side can be presented in the form

$$-2\partial_X L F_{\mu\alpha} F_\nu{}^\alpha \xi^\nu = 2\partial_X L F_\mu{}^\alpha \partial_\alpha \Phi = 2\nabla_\alpha (\Phi \partial_X L F_\mu{}^\alpha). \quad (69)$$

In this way we obtain

$$\begin{aligned} \tilde{M}_B = 2TS - \frac{\Lambda}{4\pi} \int_\Sigma \xi_\mu d\Sigma^\mu - \frac{1}{2\pi} \int_\Sigma \nabla_\alpha (\Phi \partial_X L F^{\mu\alpha}) d\Sigma_\mu \\ + \frac{1}{2\pi} \int_\Sigma \mathcal{A}^4(\varphi) [2X\partial_X L - L] \xi_\mu d\Sigma^\mu. \end{aligned} \quad (70)$$

With the help of the Stokes theorem we find

$$\begin{aligned} -\frac{1}{2\pi} \int_\Sigma \nabla_\alpha (\Phi \partial_X L F^{\mu\alpha}) d\Sigma_\mu = -\frac{1}{4\pi} \int_{S_B^2} \Phi \partial_X L F^{\mu\alpha} dS_{\mu\alpha} + \frac{1}{4\pi} \int_{\mathcal{H}} \Phi \partial_X L F^{\mu\alpha} dS_{\mu\alpha} = \\ \mathcal{O}\left(\frac{1}{r_B}\right) + \frac{\Phi_H}{4\pi} \int_{\mathcal{H}} \partial_X L F^{\mu\alpha} dS_{\mu\alpha} = \mathcal{O}\left(\frac{1}{r_B}\right) + 2\Phi_{\mathcal{H}} Q \end{aligned} \quad (71)$$

where we have taken into account that at large r_B we have $\Phi(r_B) \sim 1/r_B$ and that the electric potential is constant on the horizon. Also, the electric charge of the black hole is given by

$$Q = \frac{1}{8\pi} \int_{\mathcal{H}} \partial_X L F^{\mu\alpha} dS_{\mu\alpha}. \quad (72)$$

Summarizing, we obtained the following relation¹³

$$\tilde{M}_B = 2TS + 2\Phi_{\mathcal{H}} Q - \frac{\Lambda}{4\pi} \int_\Sigma \xi_\mu d\Sigma^\mu + \frac{1}{2\pi} \int_\Sigma \mathcal{A}^4(\varphi) [2X\partial_X L - L] \xi_\mu d\Sigma^\mu \quad (73)$$

which holds up to terms of order $\mathcal{O}(r_B^{-1})$. Having this important relation we can go back to computation of the Euclidean action. Using the field equations the bulk term can be presented in the form

$$I_{\text{bulk}} = -\frac{\Lambda}{8\pi} \int_{\mathcal{M}} \sqrt{g} d^4x - \frac{1}{4\pi} \int_{\mathcal{M}} \mathcal{A}^4(\varphi) (2X\partial_X L - L) \sqrt{g} d^4x. \quad (74)$$

Using symmetry along ξ the integration on the periodic coordinate is performed directly and we find

¹³This relation can be considered as some kind of generalized Smarr-like relation. As it was discussed in [12], in the case of nonlinear electrodynamics (at least simple) Smarr relations do not exist.

$$I_{\text{bulk}} = -\frac{\beta\Lambda}{8\pi} \int_{\mathcal{M}} \xi_\mu d\Sigma^\mu - \frac{\beta}{4\pi} \int_{\mathcal{M}} \mathcal{A}^4(\varphi)(2X\partial_X L - L)\xi_\mu d\Sigma^\mu. \quad (75)$$

At this stage we should make use of the relation (73) which gives

$$\frac{I_{\text{bulk}}}{\beta} = \frac{1}{2}\tilde{M}_B - TS - \Phi_{\mathcal{H}}Q \quad (76)$$

up to terms of order $\mathcal{O}(r_B^{-1})$. Direct computations of the other Euclidean terms give the following results

$$\frac{I_{\Theta}}{\beta} = \frac{3}{2}M - r_B - \frac{3}{2}\frac{r_B^3}{\ell^2}, \quad (77)$$

$$\frac{I_{\text{ct}}}{\beta} = -M + r_B + \frac{r_B^3}{\ell^2}, \quad (78)$$

$$\frac{I_{\text{cf}}}{\beta} = \Phi_{\mathcal{H}}Q, \quad (79)$$

up to terms of order of $\mathcal{O}(r_B^{-1})$. So for the Euclidean action, up to terms of order of $\mathcal{O}(r_B^{-1})$, we find

$$\frac{I}{\beta} = \frac{1}{2}\tilde{M}_B + \frac{1}{2}M - \frac{1}{2}\frac{r_B^3}{\ell^2} - TS. \quad (80)$$

Finally, making use of (65) we obtain

$$\frac{I}{\beta} = M - TS + \mathcal{O}\left(\frac{1}{r_B}\right) \quad (81)$$

which shows that in the limit $r_B \rightarrow \infty$ we indeed have $I/\beta = M - TS$. Let us note that the above considerations hold for arbitrary nonlinear electrodynamics not only for the Born-Infeld electrodynamics.

C Off-shell considerations

Let us consider different black holes, with different masses and entropies¹⁴, placed in a thermostat where the role of the thermostat is played by the Hawking radiation and the appropriate boundary conditions. Then we could ask which black holes would be

¹⁴In the field black-hole thermodynamics it is usually accepted to work with the radius of the event horizon instead of the entropy.

in equilibrium with the thermostat. The equilibrium black holes, or in other words the equilibrium states are those for which the off-shell¹⁵ free energy

$$F_{\text{off}} = M - T_{\text{th}}S, \quad (82)$$

has an extremum. In the above expression T_{th} is the temperature of the thermostat, it is kept fixed, and S and M are, respectively, the entropy and the mass of a black hole with radius of the event horizon r_H . The off-shell free energy for several values of T_{th} is given in Figs. 21 and 22.

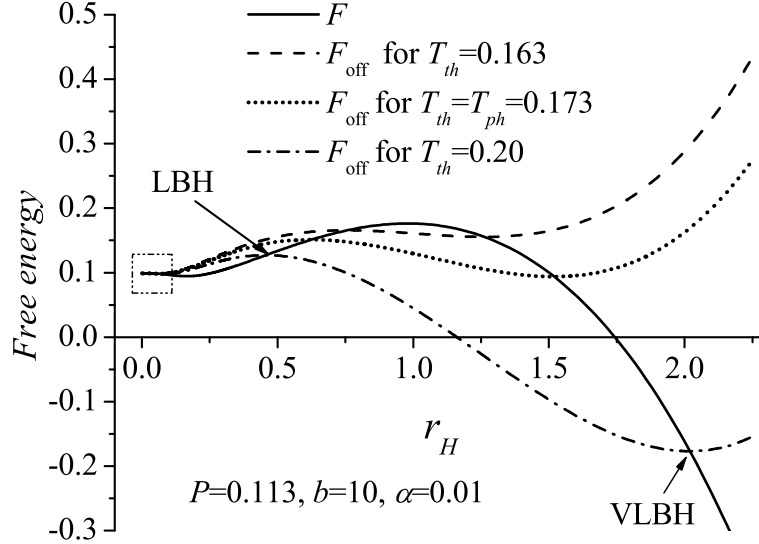


Figure 21: The free energy F for sequence of black hole solution and the off-shell free energy F_{off} for several different temperatures of the thermostat T_{th} as functions of the radius of the event horizon r_H .

The equilibrium black holes have temperature of the horizon T that is equal to the temperature of the thermostat T_{th} . The different extrema are, actually, the different phases of the system. The free energy of the different phases, namely, the equilibrium black holes, is plotted with a thick line in Figs. 21 and 22 and it intersects F_{off} in its extrema. The stable phases are in the minima and the unstable in the maxima of F_{off} . The system is in the phase that realizes a global minimum of F_{off} . A phase transition occurs when with the varying of the temperature of the thermostat T_{th} the system passes from one minimum to another. The different branches of the equilibrium free energy F as a function of the temperature of the event horizon T (see, for example, the right panel of Fig. 17) can be obtained in the following way. As we know, the thermodynamic parameters, in our case the temperature and the radius of the black hole, are independent variables. They are related only at equilibrium, i.e. at an

¹⁵This energy is actually the off-equilibrium energy. The term off-shell is used to emphasize that it is not the natural free energy connected with the solutions. The on-shell energy, the one related with the solutions, is defined in the same way but T_{th} is substituted with the temperature of the event horizon T , which is different for black holes with different r_H .

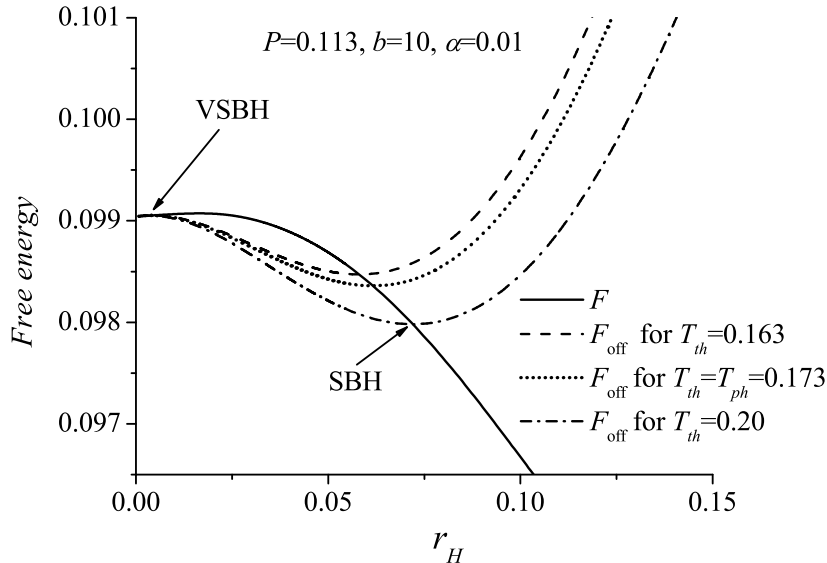


Figure 22: Magnification of the enclosed region in Fig. 21

extremum of the off-shell free energy. The condition for an extremum of F_{off} is

$$\left. \frac{\partial F_{\text{off}}(r_H)}{\partial r_H} \right|_{T_{\text{th}}=\text{const}} = 0 \quad (83)$$

This relation defines r_H as an implicit function of T_{th} which, in the general case, may have several branches $r_{H,a}(T_{\text{th}})$, $a = 0, 1, 2, \dots$. When we take into account that at equilibrium $T = T_{\text{th}}$ we obtain the $r_H - T$ diagram (see, for example, the left panel of Fig. 17). As we can see, the number of the extrema of F_{off} for a given fixed value of T coincides with the number of branches of the $r_H - T$ diagram for $T = T_{\text{th}}$ and the positions of the extrema coincide with the radii of the event horizon of the different branches.

The different branches of the on-shell or the equilibrium free energy (see, for example, the right panel of Fig. 17) can be obtained from the off-shell energy in the following way:

$$F_a(T) = F_{\text{off}}(r_{H,a}(T_{\text{th}}), T_{\text{th}})|_{T_{\text{th}}=T}. \quad (84)$$

Let us consider, for example, black holes with $P = 0.113$. As can be seen in Fig. 21 for $T_{\text{th}} = 0.173$ the minimum corresponding to SBH and the one corresponding to VLBH are equal so this is the temperature of the phase transition T_{ph} .

The off-shell formalism can give also a very transparent description of the zeroth-order phase transition that occurs in the subinterval of the magnetic charge $P_{\text{ph}}^{(1)} < P < P_{\text{ph}}^{(2)}$. The off-shell free energy is plotted in Fig. 23. The right panel is a magnification of the enclosed region in the left panel of the same figure. The three curves correspond to temperatures belonging, respectively, to the three intervals $T_0 < T < T_{\text{min}}$, $T_{\text{min}} < T < T_{\text{ph}}$ and $T_{\text{ph}} < T$. It can be seen that for $T_0 < T < T_{\text{min}}$ the off-shell free energy has only two extrema – one minimum and one maximum¹⁶. Hence, in that temperature

¹⁶Notice that the on-shell free energy intersects the curve of the off-shell free energy only at two

interval only one locally stable phase is present – the VLBH. For temperatures in the interval $T_{\min} < T < T_{\text{ph}}$ a second minimum of the off-shell free energy corresponding to SBH occurs. It is lower than the minimum corresponding to the VLBH so the SBH is thermodynamically favored. As we have already mentioned the phase transition from the VLBH to SBH that occurs at $T = T_{\min}$ is of zeroth order. As can be seen in Fig. 23, in the last temperature interval $T_{\text{ph}} < T$ the ensemble is again dominated by the VLBH since its minimum is lower than the minimum corresponding to the SBH and at the point $T = T_{\text{ph}}$ first order phase transition occurs.

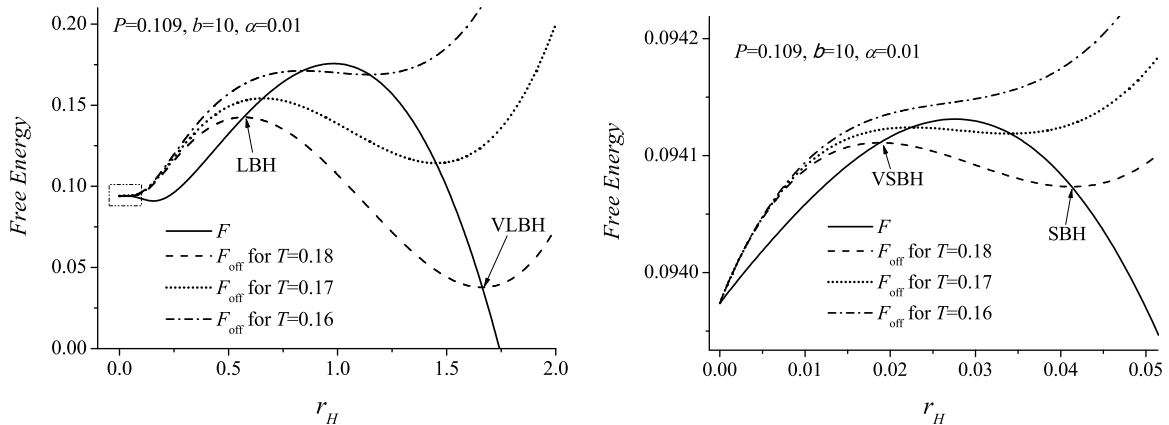


Figure 23: The off-shell free energy for the case of the zeroth-order phase transition. The right panel is a magnification of the enclosed region of the left panel of the figure.

References

- [1] J. Maldacena, *Adv. Theor. Math. Phys.* **2**, 231 (1998); arXiv: hep-th/9711200.
- [2] J. L. Petersen, *Int. J. Mod. Phys. A* **14**, 3597 (1999) ; arXiv: hep-th/9902131
- [3] S. W. Hawking and D. N. Page, *Commun. Math. Phys.* **87**, 577 (1983).
- [4] M. Born and L. Infeld, *Proc. R. Soc. London* **A143**, 410 (1934).
- [5] E. Fradkin and A. Tseytlin, *Phys. Lett.* **B 163**, 123 (1985).
- [6] E. Bergshoeff, E. Sezgin, C. Pope and P. Townsend, *Phys. Lett.* **B 188**, 70 (1987).
- [7] R. Metsaev, M. Rahmanov, and A. Tseytlin, *Phys. Lett.* **B 193**, 207 (1987).
- [8] R. Leigh, *Mod. Phys. Lett. A* **4**, 2767 (1989).
- [9] D. L. Wiltshire, *Phys. Rev.* **D 38**, 2445 (1988).
- [10] H. P. de Oliveira, *Class. Quantum Grav.* **11**, 1469 (1994).

points.

- [11] G. Gibbons and D. Rasheed, *Nucl. Phys.* **B 454**, 185 (1995).
- [12] D. Rasheed, arXiv: hep-th/9702087.
- [13] E. Ayón-Beato and A. García, *Phys. Rev. Lett.* **80**, 5056 (1998)
- [14] M. Novello, S. Perez Bergliaffa and J. Salim, *Class. Quantum Grav.* **17**, 3821 (2000).
- [15] K. Bronnikov, *Phys. Rev.* **D 63**, 044005 (2001).
- [16] G. W. Gibbons and C. A. R. Herdeiro, *Class. Quant. Grav.* **18**, 1677 (2001).
- [17] T. Tamaki and T. Torii, *Phys. Rev.* **D 64**, 024027 (2001).
- [18] A. Burinskii and S. R. Hildebrandt, *Phys. Rev.* **D 65**, 104017 (2002).
- [19] M. Gürses and Ö. Sarioglu, *Class. Quantum Grav.* **20**, 351 (2003).
- [20] N. Breton and R. Garcia-Salcedo, Contributed chapter to book on nonlinear electrodynamics edited by CBPF (Brazil); arXiv: hep-th/0702008.
- [21] A. García, H. Salazar and J. Plebański, *Nuovo Cimento Soc. Ital. Fis.* **B 84**, 65 (1984).
- [22] M. Demianski, *Found. Phys.* **16**, 187 (1986).
- [23] G. Clement and D. Gal'tsov, *Phys. Rev.* **D 62**, 124013 (2000).
- [24] T. Tamaki and T. Torii, *Phys. Rev.* **D 62**, 061501 (2000).
- [25] R. Yamazaki and D. Ida, *Phys. Rev.* **D 64**, 024009 (2001).
- [26] N. Breton; arXiv: gr-qc/0109022
- [27] S. Yazadjiev, P. Fiziev, T. Boyadjiev and M. Todorov, *Mod. Phys. Lett.* **A 16**, 2143 (2001).
- [28] S. Fernando and D. Krug, *Gen. Relat. Grav.* **35**, 129 (2003).
- [29] N. Breton, *Phys. Rev.* **D 67**, 124004 (2003).
- [30] T. Tamaki, *J. Cosm. Astr. Phys.* **0405**, 004 (2004).
- [31] T. Kumar Dey, *Phys. Lett.* **B 595**, 484 (2004).
- [32] R. Cai, D. Pang and A. Wang, *Phys. Rev.* **D70**, 124034 (2004).
- [33] M. Aiello, R. Ferraro and G. Giribet, *Phys. Rev.* **D 70**, 104014 (2004).
- [34] S. Yazadjiev, *Phys. Rev.* **D 72**, 044006 (2005).
- [35] A. Sheykhi, N. Riazi and M. H. Mahzoon, *Phys. Rev.* **D 74**, 044025 (2006).

- [36] Xian Gao, *JHEP* **0711**, 006 (2007).
- [37] Sangheon Yun, arXiv: 0706.2046.
- [38] I. Stefanov, S. Yazadjiev and M. Todorov, *Phys. Rev.* **D 75**, 084036 (2007).
- [39] I. Stefanov, S. Yazadjiev and M. Todorov, *Mod. Phys. Lett.* **22** (17), 1217 (2007).
- [40] A. Sheykhi, *Phys. Lett.* **B 662**, 7 (2008).
- [41] S. Fernando, *Phys. Rev.* **D 74**, 104032 (2006).
- [42] A. Sheykhi, N. Riazi, *Phys. Rev.* **D 75**, 024021 (2007).
- [43] W. A. Chamissany, Mees de Roo, S. Panda, *Class. Quant. Grav.* **25**, 225009 (2008).
- [44] A. Sheykhi, *Int. J. Mod. Phys.* **D 18**, 25 (2009); arXiv: 0801.4112.
- [45] C. M. Will, “*The Confrontation between General Relativity and Experiment*”, *Living Rev. Relativity* **9**, 3 (2006), URL (cited on 10.11.2009): <http://www.livingreviews.org/lrr-2006-3>, arXiv:gr-qc/0103036.
- [46] I. Stefanov, S. Yazadjiev and M. Todorov, *Mod. Phys. Lett.* **A 23** (34), 2915 (2008), arXiv: 0708.4141.
- [47] Yun Soo Myung, Yong-Wan Kim and Young-Jai Park, *Phys. Rev.* **D 78**, 084002 (2008); arXiv: 0805.0187.
- [48] A. Chamblin, R. Emparan, C. V. Johnson, R. C. Myers, *Phys.Rev.* **D 60**, 064018 (1999); arXiv: hep-th/9902170.
- [49] A. Chamblin, R. Emparan, C. V. Johnson, R. C. Myers, *Phys.Rev.* **D 60**, 104026 (1999); arXiv:hep-th/9904197.
- [50] Yun Soo Myung, *Mod. Phys. Lett.* **A 23**, 667 (2008).
- [51] Yun Soo Myung, *Phys. Lett.* **B 663**, 111 (2008).
- [52] T. Kumar Dey, S. Mukherji, S. Mukhopadhyay and S.Sarkar, *JHEP* **0704**,014 (2007).
- [53] T. Kumar Dey, S. Mukherji, S. Mukhopadhyay and S.Sarkar, *JHEP* **0709**,026 (2007).
- [54] Cho Y. M. Cho and Ishwaree P. Neupane, *Phys. Rev.* **D 66** , 024044 (2002).
- [55] H. A. Gonzalez, M. Hassaine and C. Martinez, *Phys. Rev.* **D 80**, 104008 (2009); *CECS-PHY-09/08* ; arXiv:0909.1365 [hep-th].
- [56] S. Stotyn and R. Mann, *Phys. Lett.* **B 681**, 472 (2009); arXiv:0909.0919 [hep-th].
- [57] G. Gibbons and D. Rasheed, *Nucl. Phys.* **B454**, 185 (1995).

- [58] G. Gibbons and D. Rasheed, *Phys.Lett.* **B365**, 46 (1996).
- [59] Humberto Salazar I., Alberto García D. and Jerzy Plebański, *J. Math. Phys.* **28**(9), 2171 (1987).
- [60] K. Bronnikov, *Phys. Rev.* **D63**, 044005 (2001).
- [61] Paolo Aschieri, Sergio Ferrara and Bruno Zumino, *Riv.Nuovo Cim.* **31**, 625 (2008); arXiv: 0807.4039 [hep-th] (2008).
- [62] M. K. Gavurin, *Izvestia VUZ, Matematika* **14**(6), 18–31 (1958) (in Russian) (see also *Math. Rev.* **25**, 1380 (1963)).
- [63] E. P. Jidkov, G. I. Makarenko and I. V. Puzynin, in *Physics of Elementary Particles and Atomic Nuclei* (JINR, Dubna, 1973) vol. 4, part I, 127–166 (in Russian), English translation: *American Institute of Physics*, p.53.
- [64] T. L. Boyadjiev, M. D. Todorov, P. P. Fiziev and S. S. Yazadjiev, *J. Comp. Appl. Math.* **145**(1), 113 (2002); arXiv: math/0004108 [math.NA].
- [65] V. Balasubramanian and P. Kraus, *Commun. Math. Phys.* **208**, 413 (1999).
- [66] G. Arcioni and E. Lozano-Tellechea, *Phys.Rev.* **D 72**, 104021 (2005).
- [67] H. J. de Vega and N. S'anchez, *Nucl. Phys.* **B 625**, 409 (2002), arXiv: astro-ph/0101568.
- [68] S. Bustingorry, E. A. Jagla and J. Lorenzana, *Acta Materialia*, **53**, Issue 19, 5183 (2005); arXiv: cond-mat/0509489 (see also arXiv: cond-mat/0307134) .
- [69] V. Maslov, *Theor. and Math. Phys.* **150**, 102 (2007).
- [70] D. Doneva, S. Yazadjiev, K. Kokkotas, I. Stefanov and M. Todorov, paper in preparation
- [71] M. Cadoni, G. D'Appollonio and P. Pani, *J. High Energy Phys.* **03** (2010) 100; arXiv: 0912.3520 [hep-th].
- [72] G. Kang, *Phys. Rev.* **D54**, 7483 (1996).
- [73] M. Visser, *Phys. Rev.* **D48**, 583 (1993).
- [74] T. Jacobson, G. Kang and R. Myers, *Phys. Rev.* **D52**, 3518 (1995).
- [75] L. H. Ford and Thomas A. Roman, *Phys. Rev.* **D64**, 024023 (2001).
- [76] T. Jacobson and G. Kang, *Class. Quant. Grav.* **10** L201 (1993).
- [77] D. L. Lee, *Phys. Rev.* **D10**, 2374 (1974).
- [78] M. A. Scheel, S. L. Shapiro, and S. A. Teukolsky, *Phys. Rev.* **D 51**, 4208 (1995).

- [79] A. W. Whinnett, *Class. Quantum Grav.* **16**, 2797 (1999).
- [80] S. S. Yazadjiev, *Class. Quantum Grav.* **16**, L63 (1999).
- [81] R.B. Mann, *Phys. Rev. D* **60**, 104047 (1999); *Phys. Rev. D* **61**, 084013 (2000).